PHILOSOPHICAL TRANSACTIONS OF THE ROYAL SOCIETY A MATHEMATICAL, PHYSICAL & ENGINEERING SCIENCES

Subsidence due to Pumping from a Soil Stratum with a Soft Aquitard

Cheo K. Lee, Sophie N. Fallou and Chiang C. Mei

Phil. Trans. R. Soc. Lond. A 1992 **339**, 193-230
doi: 10.1098/rsta.1992.0032

Subsidence due to pumping from a soil stratum with a soft aquitard

By Cheo K. Lee, Sophie N. Fallou and Chiang C. Mei

Parsons Laboratory for Water Resources and Hydrodynamics, Department of Civil Engineering, Massachusetts Institute of Technology, Cambridge, Massachusetts 02139, U.S.A.

Contents

Phil. Trans. R. Soc. Lond. A (1992) **339**, 193–230
Printed in Great Britain

We examine theoretically the mechanics of intensive pumping of groundwater from a layered soil. The soil system is assumed to consist of three horizontal layers where a very soft and highly impervious aquitard is sandwiched by two hard and highly porous aquifers. Water is pumped from the bottom aquifer through a vertical well. Attention is focused on the case where the pumping rate is so strong that the ground subsidence, contributed mainly by the soft aquitard, is comparable with the typical layer thickness. By a perturbation theory and the use of lagrangian coordinates, we deduce an approximation which incorporates the quasi-three-dimensional scheme of Hantush & Jacob for the pore pressure, and the one-dimensional finite strain theory of Gibson *et al.* for the soil consolidation. Unlike the approximations prevailing in hydrological literature, it is shown in particular that the pore pressure is nonlinearly coupled to the soil deformation and that the total stress is not necessarily uniform in depth. Hysteretic subsidence and the associated variations of soil parameters due to various forms of cyclic pumping or recharging are discussed.

1. Introduction

Groundwater is frequently pumped from confined aquifers of a soil stratum consisting of alternating layers of highly porous sand (aquifers) and highly impervious clay (aquitards). Many existing works are based on Biot's linearized equations of poroelasticity. Since fully three-dimensional problems coupling several soil layers are prohibitively complex, it is often assumed that the total stress, which is the sum of the effective soil stress and the pore pressure, does not vary with depth in a soil layer (see Verruijt 1969). As a consequence, the soil dilation rate is then proportional to the pore pressure. This leads to a linear diffusion equation for the incremental pore pressure (or drawdown) which is decoupled from the soil deformation,

$$k\nabla^2 s = (\rho s/D)\,\partial s/\partial t, \tag{1.1}$$

where s = drawdown, k = permeability, and D = elastic modulus of matrix. However, this assumption is known to hold only if the consolidating layer is sufficiently thin and hard (De Josselin de Jong 1963), as can be inferred from the one-dimensional consolidation theory of a soft and thick clay layer by Gibson *et al.* (1967) and by Gibson *et al.* (1981).

In some theories of multilayer subsidence, soil deformation is attributed mainly to the aquifers (see Verruijt 1969; Bredehoeft & Pinder 1970; Corapcioglu & Brutsaert 1977; Bear & Corapcioglu 1981*a*, *b*; Corapcioglu & Bear 1983). The aquitards are treated as relatively thin but firm lens across which there is a pressure drop. However, it is known that aquitards themselves may also play an important role in subsidence because of the relatively large compressibility of some clays (Poland & Davis 1969; Gambolati & Freeze 1973; Gambolati *et al.* 1974; Helm 1975, 1976; Narasimhan & Witherspoon 1977, 1978). In a pioneering study of pumping from a single well, Hantush & Jacob (1955*a*, *b*; Hantush 1960) introduced a model which accounts for compaction in the aquitards for a soil system with three alternating sand and clay layers, with water pumped out of the bottom (artesian) aquifer. From the simple case of steady flow in two layers with very different permeabilities (Hantush & Jacob 1954, 1955*b*; Bear 1972, p. 157), they invoked the following approximation which captures much of the essential physics. First, the flow in an aquifer should be nearly horizontal because of the relatively high permeability, and its depth-average is governed by

$$b\left(\frac{\partial^2}{\partial x^2}+\frac{\partial^2}{\partial y^2}\right)\bar{s}+\left[\frac{\partial s}{\partial z}\right]_-^+=\frac{\rho g b}{kD}\frac{\partial \bar{s}}{\partial t}, \tag{1.2}$$

where b and $\bar{s}$ are the aquifer thickness and the depth-averaged aquifer drawdown respectively and D is the constrained modulus, and

$$\left[\frac{\partial s}{\partial z}\right]_-^+=\frac{\partial s}{\partial z}\bigg|_+-\frac{\partial s}{\partial z}\bigg|_-=\frac{\partial s_+}{\partial z}-\frac{\partial s_-}{\partial z} \tag{1.3}$$

is proportional to the net flux into the aquifer from the aquitard immediately above and below. Second, the flow in the highly impermeable aquitard must be nearly vertical, hence $\partial s/\partial z \gg \partial s/\partial x$, $\partial s/\partial y$ so that (1.1) in the upper (+) aquitard is approximately governed by a vertical diffusion equation

$$\frac{\partial^2 s_+}{\partial z^2}=\frac{\rho g}{k_+ D_+}\frac{\partial s_+}{\partial t}. \tag{1.4}$$

The lower aquitard is governed by a similar equation. Thus the original problem in three dimensions becomes one dimensional (vertical) in the aquitard and two dimensional (horizontal) in the aquifer. This quasi-three-dimensional hydrological approximation significantly eases the computational task and has been the basis of many later extensions (Herrera & Figueroa 1969; Neuman & Witherspoon 1969*a*, *b*; Gambolati *et al.* 1986; see Fallou *et al.* (1991) for an extensive list of references). It has been shown for a numerical example to be highly accurate as long as the permeability contrast is sufficiently great (Javandel & Witherspoon 1969). After obtaining the three-dimensional pore pressure, the soil deformation is taken to be one dimensional. The assumption of constant total stress then gives the effective stress from the local pore pressure. A linear or nonlinear constitutive law between the effective stress and strain (or void ratio) is introduced at this stage to obtain the ground subsidence. Examples of this scheme include Gambolati & Freeze (1973), Gambolati *et al.* (1974) for Venice, Italy. To simulate the recorded subsidence of Pixley, California, Helm (1975, 1976) and Narasimhan & Witherspoon (1977, 1978) used a strictly one-dimensional model with prescribed load on the ground surface. Hysteretic soil behaviour under cyclic or intermittent loading was examined. The effects of partial saturation were further included in Narasimhan & Witherspoon. For the three-dimensional problem of pumping from the bottom aquifer of a three-layered system, Rudolph & Frind (1991) considered the aquitard to be highly compressible. With the hydrological approximation corresponding to (1.2) to (1.4), they introduced nonlinear empirical relations between k, D and the soil effective stress and void ratio which are in turn related by an empirical law. However, they formulated the mathematical problem for the aquitard in a fixed domain therefore assumed in effect that the depth of the aquitard is unchanged during consolidation. This is not fully consistent with the assumption of high compressibility which implies in general that the position of the upper boundary of the aquitard is unknown *a priori*. In Mexico City where the soil consists of many clay strata of a few to few tens of metres thick, alternating with sand and gravel layers, it is known that the total subsidence since 1880 is as high as 7 m (Bolt *et al.* 1977; Zeevaert 1983).

Towards a more complete theory for a soil system with a soft and thick aquitard, the following issues warrant re-examination. (i) Is the total stress in the aquitard always constant in depth? (ii) How is the finite strain of the soil matrix coupled

PHILOSOPHICAL TRANSACTIONS OF THE ROYAL SOCIETY A MATHEMATICAL, PHYSICAL & ENGINEERING SCIENCES

with the drawdown? (iii) How does the water table evolve if the unpumped aquifer on the top is unconfined? (iv) To what extent is the quasi-three-dimensional approximation of Hantush & Jacob valid in the nonlinearly coupled problem?

To provide partial answer to (i) and (iii) above, Fallou *et al.* (1991) have recently applied a perturbation analysis to the classical problem of pumping from a single well in a three-layered system, with the top layer unconfined. Based on Biot's poroelasticity theory for weak disturbances due to pumping, they concluded analytically that while the quasi-three-dimensional picture is indeed the first approximation in a power series expansion of the small ratio of aquitard-to-aquifer permeabilities, self weight can nevertheless cause the total stress to be non-uniform in a thick soft aquitard.

For strictly one-dimensional consolidation, large deformation can be most elegantly dealt with by a lagrangian approach introduced by Cooper (1966, with revisions by Gambolati (1973*a*, *b*)), Gibson *et al.* (1967) and Smiles & Rosenthal (1968). This approach allows one to follow the finite displacement of the soil matrix in the most direct manner, but it needs to be extended for the general case of three dimensions.

In this paper we use the classical example of pumping from an isolated region in a soil system consisting of three horizontal layers of comparable thickness, with an aquitard sandwiched between two aquifers. All layers are infinite in radial extent. Lagrangian coordinates will be used. Rather than invoking the hydrological approximation of Hantush & Jacob heuristically, we shall extend our perturbation theory for small permeability ratio (aquitard to aquifer), to deduce a similar simplification for the flow. (We are following a philosophy well known in the modern theory of shallow water waves, in which Airy's original heuristic approximation can be derived as the leading-order approximation in a formal perturbation analysis, which facilitates extentions to higher orders.) We also show that the one-dimensional lagrangian theory for the soil matrix is still valid to certain degree of accuracy. To facilitate the explanation of our analysis, we do not include all physical factors that may be present in some circumstances, but retain those essential for our argument. Thus the compressibility of water and partial saturation are neglected. The aquifers are assumed to be very much more rigid than the aquitard. The sharp phreatic surface will be found as a part of the nonlinear solution. In addition to ground subsidence, we also examine the variations of the soil parameters as functions of the pumping rate. Several types of steady and transient pumping schedules are discussed.

In §2, after listing the governing equations for quasi-static states, constitutive assumptions are introduced. The well-known hysteretic relation between compression and the void ratio will be schematized by one involving just two coefficients; modification for any particular soil should be minor. To provide a mathematical basis for perturbation analysis, we first estimate the order of magnitudes of all physical quantities in this problem. In this process the linear Biot's theory is used only as a guide but for no other purposes. The governing equations are then normalized by these estimated scales, and dimensionless coefficients in powers of the small ratio of depth-averaged permeabilities

$$\delta = \hat{k}_2/\hat{k}_1 \ll 1 \tag{1.5}$$

appear with each term to display its relative importance in the equation. Physically the small parameter δ is also associated with the shallowness of layers. A perturbation

PHILOSOPHICAL TRANSACTIONS OF THE ROYAL SOCIETY A MATHEMATICAL, PHYSICAL & ENGINEERING SCIENCES

analysis then ensues. In §4 transformation rules from eulerian to lagrangian coordinates are discussed. In §5 it is shown that the lagrangian equation of Gibson *et al.* remains a good representation for the effective stress in the soft aquitard. In §6, the flow in the artesian aquifer is shown to be horizontal to the leading order $O(\delta^0)$, while the soil deformation is insignificant. Consideration of $O(\delta)$ leads to a boundary condition for the drawdown in the aquitard above. The mechanics in the phreatic aquifer involves significant displacement of the water table. Perturbation analysis in §7 based on lagrangian coordinates gives another boundary condition on the upper interface for the aquitard drawdown. In this way the mathematical problem for three layers is reduced to one for the aquitard alone. The aquitard equation is then rewritten for the aquitard drawdown in §8. Also formulas for other physical variables are summarized in dimensionless form in §9. For the purpose of checking the limiting case of hard aquitards is considered in §10 and it is shown that the boundary value problem for the aquitard drawdown reduces to the one by Hantush (1960) as the storage coefficient of the aquitard becomes negligible. After outlining the numerical scheme in §11, numerical results for steady and transient pumping are discussed in §12. The Mandel–Cryer effect is pointed out in which the water table near the well rises during the initial stage of pumping. Intermittent or cyclic pumping and recharging are examined for hysteretic responses in the vertical displacements of both the ground surface and the water table. Remarks for future extensions are made in §13.

2. Governing equations for deformable porous media

In this section we present the governing equations which are applicable in all soil layers. Subscripts for distinguishing the layers will not be introduced until later.

(*a*) *Conservation equations*

Let n be the porosity of the soil matrix, ρ_w and $\boldsymbol{v}_w$ the density and velocity respectively of the pore water. Conservation of water mass requires that

$$\partial n\rho_w/\partial t+\nabla\cdot(n\rho_w\boldsymbol{v}_w)=0. \tag{2.1}$$

Similarly, if ρ_s and $\boldsymbol{v}_s$ denote the density and velocity of the solid matrix, conservation of solid mass requires that

$$\partial(1-n)\rho_s/\partial t+\nabla\cdot[(1-n)\rho_s\boldsymbol{v}_s]=0. \tag{2.2}$$

In this paper, both ρ_w and ρ_s are assumed to be constant. Equations (2.1) and (2.2) can then be combined to give the so-called *storage equation*

$$\nabla\cdot[n(\boldsymbol{v}_w-\boldsymbol{v}_s)]+\nabla\cdot\boldsymbol{v}_s=0. \tag{2.3}$$

Let p be the pore pressure and k the hydraulic conductivity of the soil matrix. With inertia neglected, momentum conservation of the fluid phase is given approximately by Darcy's law

$$\nabla p=\rho_w\boldsymbol{g}-(n\rho_w g/k)(\boldsymbol{v}_w-\boldsymbol{v}_s). \tag{2.4}$$

Following a convention in ground water hydraulics, we define the *drawdown* s as the change in piezometric head from the initial state,

$$s=p/\rho_w g+z-H, \tag{2.5}$$

PHILOSOPHICAL TRANSACTIONS OF THE ROYAL SOCIETY A MATHEMATICAL, PHYSICAL & ENGINEERING SCIENCES

where H is the initial height of the water table in the phreatic aquifer, measured from the bed rock at the bottom of the whole system. In terms of s, Darcy's law becomes

$$k\nabla s = -n(\boldsymbol{v}_w - \boldsymbol{v}_s). \tag{2.6}$$

Combining (2.6) with (2.3), the storage equation may be written

$$\nabla\cdot(k\nabla s) = \nabla\cdot\boldsymbol{v}_s. \tag{2.7}$$

If the total stress tensor in the solid matrix is denoted by τ, with components τ_{ij}, the approximate equation of solid momentum conservation is, after ignoring inertia,

$$\nabla\cdot\tau = -((1-n)\rho_s + n\rho_w)\boldsymbol{g}. \tag{2.8}$$

The convention of positive tension is adopted here. Let the effective stress tensor σ, with components σ_{ij}, be defined by

$$\sigma = \tau + p\boldsymbol{I}, \tag{2.9}$$

where $\boldsymbol{I}$ is the identity tensor. Equations (2.8) and (2.9), can be combined to give

$$\nabla\cdot\sigma = \nabla p - ((1-n)\rho_s + n\rho_w)\boldsymbol{g}, \tag{2.10}$$

or, in terms of the drawdown s,

$$\nabla\cdot\sigma = \rho_w g\nabla s - (1-n)(\rho_s - \rho_w)\boldsymbol{g}. \tag{2.11}$$

Let all quantities (except depths) of the initial state before pumping starts be distinguished by the overhead bar, then,

$$\bar{s} = \bar{\boldsymbol{v}}_s = \bar{\boldsymbol{v}}_w = 0, \quad \bar{p} = \rho_w g(H-z) \tag{2.12}$$

and

$$\nabla\cdot\bar{\sigma} = \rho_w\boldsymbol{g} - [(1-\bar{n})\rho_s + \bar{n}\rho_w]\boldsymbol{g}. \tag{2.13}$$

All pumping-induced departures from the initial state will be distinguished by primes, i.e.

$$\left.\begin{aligned} &n = \bar{n}+n', \quad p = \bar{p}+p', \quad \sigma = \bar{\sigma}+\sigma', \\ &k = \bar{k}+k', \quad \boldsymbol{v}_s = \boldsymbol{v}_s', \quad \boldsymbol{v}_w = \boldsymbol{v}_w', \\ &b = B+b', \quad h = H+h', \quad s = s' = p'/\rho_w g, \end{aligned}\right\} \tag{2.14}$$

where h, H and h' are respectively the instantaneous height, the initial height and the change of height of the water table. Similarly, b, B and b' are the instantaneous thickness, the initial thickness and the change of thickness of a soil layer.

(b) *Constitutive laws for finite strain*

We are particularly interested in the response of a soft soil in which the initial state due to self weight and the transient state during pumping are expected to be one of finite strain. It will be deduced later that soil deformation in this three-dimensional problem is approximately one dimensional to the desired accuracy. Hence empirical relations between stresses and strains well established from one-dimensional tests will be relevant and will be cited here first. These relations are usually expressed for the effective stress and the void ratio e, or the porosity n, which are related by

$$e = n/(1-n), \quad \text{or} \quad n = e/(1+e). \tag{2.15}$$

One customary form of the empirical relation is

$$\mathrm{d}e = a_v\,\mathrm{d}\sigma_{zz}, \tag{2.16}$$

where the coefficient of compressibility a_v is an empirical function of e (see Lambe & Whitman 1969, p. 155). An alternative form is

$$\mathrm{d}e = -C_c\,\mathrm{d}(\log_{10}(-\sigma_{zz})) \tag{2.17}$$

where C_c is the compression index. Equations (2.16) and (2.17) can be combined to give

$$a_v(e) = -(1/\ln 10)\,C_c/\sigma_{zz}(e). \tag{2.18}$$

For virgin compression, the compression index C_c of some materials may be approximated by a constant within certain range of stresses. For cyclic loadings, C_c is often multivalued as the stress changes quasi-statically through virgin compression, swelling and recompression (see Lambe & Whitman 1969). To explore possible hysteretic responses caused by this multivaluedness, we adopt a schematized relation between e and $\log_{10}(-\sigma)$ in which virgin compression follows a straight line with constant slope C_c, and both swelling and recompression follow another straight line with a smaller slope C_c'. This schematization can be readily replaced by the actual relation for any particular soil without modifying our theory. While typical values of C_c for sand are 0.001–0.01 and 0.2–0.4 for common clays, the Mexico City clay is exceptionally soft and C_c has been variably estimated to be in the range 4.5–8 (Holtz & Kovacs 1981; Lambe 1951). Since the consolidation process is usually very slow, these quasi-static relations will be adopted for both the initial and the transient states.

Just for the order estimation of solid strains, we later refer to the linear equations of poroelasticity in terms of the constrained modulus D and the shear modulus G. In linear theories, they are related to the usual Lamé constant λ by $\lambda = D - 2G$ and to the bulk modulus β by $D = \beta + \frac{4}{3}G$. For finite soil strain the constrained modulus is related to e by

$$D = (1+e)/a_v(e). \tag{2.19}$$

(*c*) *Hydraulic conductivity*

The empirical Kozeny–Carman equation between k and e will be adopted:

$$k = \frac{\rho g}{\mu}\frac{c_0}{M_s^2}\frac{e^3}{1+e}, \tag{2.20}$$

where ρ and μ are the mass density and the viscosity of the pore fluid (Lambe & Whitman 1969, p. 287; Bear 1972). Kozeny's constant c_0 varies with the shape and size of the particles, and is of order 0.5. The specific surface M_s per unit volume of solid material is also a characteristic of porous medium. It varies from 100 cm^{-1} for coarse sands to 10^5 cm^{-1} and more for clays. The ratio $\rho g/\mu$ of the fluid weight density to its dynamic viscosity is of the order of 10^{-7} m s^{-1} for water.

Let the initial value of $\bar{e}$ be given at one reference depth within the layer; its variation $\bar{e}(z)$ throughout the layer as well as $\bar{\sigma}_{ij}(z)$, $\bar{k}(z)$, and $\bar{D}(z)$ are calculated by assuming virgin compression. Such computations and results have been made by Fallou *et al.* (1991), and will be cited later.

(*d*) *Boundary conditions*

On the horizontal bottom $\Gamma_0 : z = 0$, the bed rock is assumed to be rigid and impermeable. Let (u_1', w_1') denote the radial and vertical velocity components of the solid matrix in the lowest layer (the artesian aquifer) distinguished by subscript $(\cdot)_1$. Then,

$$u_1' = w_1' = 0 \quad \text{and} \quad \partial s_1'/\partial z = 0. \tag{2.21\,a, b, c}$$

Let the lower and upper interfaces be given respectively by $\Gamma_1 : z = b_1(r,t)$ and $\Gamma_2 : z = b_1(r,t) + b_2(r,t)$. Across each of them continuity of solid velocity, water flux and stresses is required,

$$[\boldsymbol{v}'_s]_- = [\boldsymbol{v}'_s]_+, \tag{2.22}$$

$$[k\nabla s' \cdot \boldsymbol{n}]_- = [k\nabla s' \cdot \boldsymbol{n}]_+, \tag{2.23}$$

$$[\boldsymbol{\sigma}' \cdot \boldsymbol{n}]_- = [\boldsymbol{\sigma}' \cdot \boldsymbol{n}]_+, \tag{2.24}$$

where the subscripts $[f]_-$ and $[f]_+$ stand for f measured just below and above the interface respectively. On the water table $\Gamma_H : z = h = H + h'(r,t)$, capillarity is ignored so that

$$s' = h' \quad \text{on } \Gamma_H. \tag{2.25}$$

Since the seepage flow can only be tangential to the water table we have

$$(\partial/\partial t + \boldsymbol{v}'_w \cdot \nabla)[z - h(r,t)] = 0, \tag{2.26}$$

or

$$\partial h'/\partial t + (\boldsymbol{v}'_w - \boldsymbol{v}'_s) \cdot \nabla h' + \boldsymbol{v}'_s \cdot \nabla h' - \boldsymbol{v}_w \cdot \nabla z = 0. \tag{2.27}$$

It follows after invoking Darcy's law that

$$\frac{\partial h'}{\partial t} - \frac{k_3}{n_3}\frac{\partial s'_3}{\partial r}\frac{\partial h'}{\partial r} + u'_3\frac{\partial h'}{\partial r} = -\frac{k_3}{n_3}\frac{\partial s'_3}{\partial z} + w'_3, \quad \text{on} \quad \Gamma_H. \tag{2.28}$$

In addition

$$[\boldsymbol{\sigma}' \cdot \boldsymbol{n}]_- = [\boldsymbol{\sigma}' \cdot \boldsymbol{n}]_+ \quad \text{on } \Gamma_H. \tag{2.29}$$

The ground surface, $\Gamma_3 : z = b_1 + b_2 + b_3$, is assumed to be stress free

$$\boldsymbol{\sigma}' \cdot \boldsymbol{n} = 0 \quad \text{on } \Gamma_3. \tag{2.30}$$

We schematize the pumping region by a vertical well of radius a into which water is extracted only from the bottom aquifer, at the total rate of Q,

$$\int_0^{b_1} 2\pi a k_1 \frac{\partial s'_1}{\partial r}\,\mathrm{d}z = Q(t), \quad r = a, \quad 0 < z < b_1. \tag{2.31}$$

No water is pumped from the top aquifer,

$$\partial s'_3/\partial r = 0, \quad r = a, \quad b_1 + b_2 < z < h. \tag{2.32}$$

Finally all velocity components must vanish at $r \to \infty$.

3. Estimates of order of magnitude

As a basis of perturbation analysis we first establish the order of magnitude of all physical variables, under certain prescribed conditions. The generic symbol $\hat{f}$ will be used to denote the scale of any quantity f. To estimate solid deformation we use the linearized Biot theory of poroelasticity based on Hooke's law, with the elastic coefficients already defined in §2*b*. For this limited purpose Biot's equations are cited in Appendix A.

(*a*) *Drawdown*

Near the well the radial length scale is a. From the discharge boundary condition at the well, we get the scale relation

$$2\pi \hat{b}\hat{k}_1 \hat{s}_1 = \hat{Q}, \tag{3.1}$$

where $\hat{b}$ is the common thickness scale for all three layers. The order of magnitude $\hat{s}_1$ is, therefore,

$$\hat{s}_1 = O((1/2\pi)\,\hat{Q}/\hat{b}\hat{k}_1). \tag{3.2}$$

Continuity of pressure across the interfaces Γ_1 and Γ_2 implies

$$\hat{s}_1 = \hat{s}_2 = \hat{s}_3 = \hat{s}. \tag{3.3}$$

(*b*) *Horizontal length scale and the radius of influence*

Let $\hat{r}$ be the radial scale of the cylindrical zone which is significantly affected by pumping. By mass conservation, water pumped into the cylindrical region is the sum of downward leakage from the aquitard through a disc of radius $O(\hat{r})$, and the radial flow in the artesian aquifer. In general, all three rates are comparable, hence

$$2\pi \int_0^{\hat{r}} k_2 \frac{\partial s_2'}{\partial z} r\,\mathrm{d}r = O(\hat{Q}). \tag{3.4}$$

It follows from (3.3) and (3.4) that

$$\hat{b}/\hat{r} = (k_2/k_1)^{\frac{1}{2}}. \tag{3.5a}$$

The typical hydraulic conductivity of sand k_1 is of the order 10^{-2}–10^{-7} m s^{-1}, while that of clay k_2 varies between 10^{-9} and 10^{-12} m s^{-1}. Thus k_2/k_1 varies over a broad range of very small values 10^{-10}–10^{-2} and implies shallowness. This fact is well known in well hydraulics (Bear 1979), where the quantity $\hat{r}$ is called the *radius of influence*. We use the small parameter δ defined in (1.1):

$$\delta = \hat{k}_2/\hat{k}_1 = O(k_2/k_1) = O(\hat{b}/\hat{r})^2 \tag{3.5b}$$

to gauge all small quantities, where $\hat{k}_1$ and $\hat{k}_2$ are the depth averages of k_1 and k_2. Note that, if the aquitard is perfectly impermeable, then $\hat{r}/\hat{b} \to \infty$. Without seepage flow the aquitard would not experience compaction and could only settle by following bodily the deformation of the supporting aquifer.

In some situations, the horizontal length scale may be different from the hydraulic radius. For example, if a town withdraws water from an aquifer through densely distributed wells, then the horizontal dimension of the town should be taken to be $\hat{r}$. In that case, the usually small ratio $\hat{b}/\hat{r}$ is not related to the conductivity ratio as it is here.

(*c*) *Solid velocity*

As may be expected intuitively, the radial movement of the solid matrix is almost everywhere much smaller than the vertical movement. This can be seen from the linearized momentum equation in the radial direction (A 5) cited in Appendix A. By balancing the dominant terms $(\partial/\partial z)\,G\,\partial u'/\partial z$ and $\rho_w g\,\partial s'/\partial r\,\partial t$ in the radial equation (A 6) and similarly $(\partial/\partial z)\,D\,\partial w'/\partial z$ and $\rho_w g\,\partial^2 s'/\partial z\,\partial t$ in the vertical equation (A 7), we find, in each layer,

$$\hat{u}_i/\hat{w}_i = O(\hat{b}/\hat{r}) = \delta^{\frac{1}{2}}, \quad i = 1, 2, 3. \tag{3.6}$$

From the vertical component of Darcy's law, (2.6), we infer that

$$w_2' = O(k_2\,\partial s_2'/\partial z), \tag{3.7}$$

thus the following scale relation holds

$$\hat{w}_2 \sim k_2 \hat{s}/\hat{b} \sim (\hat{k}_2/\hat{k}_1)\,\hat{Q}/\hat{b}^2. \tag{3.8}$$

By continuity of displacements, we must have

$$\hat{w}_2 \sim \hat{w}_3 \sim \hat{w}. \tag{3.9}$$

To highlight the importance of the soft aquitard to consolidation we make the simplifying assumption that the aquifers are much harder so that

$$\hat{D}_2/\hat{D}_i = O(\delta^{\frac{1}{2}}), \tag{3.10}$$

where $\hat{D}_i$, $i = 1, 3$ and $\hat{D}_2$ are the depth-averages and also the scales of constrained moduli in the aquifers and the aquitard respectively. Under this assumption the velocity variations in the hard aquifers are much smaller than the velocities themselves. Indeed by using Hooke's law again only for scale estimates, we invoke stress continuity at the interfaces to get

$$\Delta\hat{w}_i/\Delta\hat{w}_2 = O(\hat{D}_2/\hat{D}_i) = O(\delta^{\frac{1}{2}}) \quad (i = 1, 3). \tag{3.11}$$

Thus the vertical compaction in the aquitard is, in general, greater by a factor of $\delta^{-\frac{1}{2}}$ than those in the aquifers. It should be emphasized that $\hat{w}_3$ and $\Delta\hat{w}_3$ of the top aquifer are not of the same order, since $w_3 = w_2$ at the interface Γ_2. This distinction is the consequence of (3.10) and is important for later analysis. For the bottom aquifer, however, this distinction disappears since $w_1 = 0$ on $z = 0$, thus

$$\hat{w}_1 = \Delta\hat{w}_1 = O(\delta^{\frac{1}{2}})\,\Delta\hat{w}_2 = O(\delta^{\frac{1}{2}})\,\hat{w}_2. \tag{3.12}$$

(d) *Consolidation timescale and storage coefficient*

Because of its relatively low permeability and high compressibility, the aquitard must control the timescale of consolidation. Again we use Hooke's law only for scale estimation, then in the vertical momentum equation for the aquitard (equation (A 7)), the two dominant terms are

$$\rho_w g \frac{\partial^2 s_2'}{\partial z\,\partial t} \quad \text{and} \quad \frac{\partial}{\partial z}\left(D_2 \frac{\partial w_2'}{\partial z}\right). \tag{3.13}$$

The timescale $\hat{t}$ can therefore be estimated by balancing them,

$$\hat{t} = \frac{\rho_w g \hat{b}}{\hat{D}_2}\frac{\hat{s}}{\hat{w}} = \frac{\rho_w g \hat{b}^2}{\hat{D}_2 \hat{k}_2} = \frac{\mathscr{S}_T \hat{b}}{\hat{k}_2} = \frac{\mathscr{S}_T \hat{s}}{\hat{w}}, \tag{3.14}$$

where $\mathscr{S}_T$ is defined by

$$\mathscr{S}_T = \rho_w g \hat{b}/\hat{D}_2. \tag{3.15}$$

The parameter $\mathscr{S}_T$ is called the *storage coefficient* in hydrology and is physically associated with gravity or self weight. In existing literature (Verruijt 1969) gravity is often omitted in the vertical balance of forces. In one dimension, the total stress $\sigma_{zz} - p$ is constant in depth. Let us recall (2.10) and examine the effect of such omission in the aquitard. After subtracting the static terms we get

$$n'(\rho_s - \rho_w)\, g = O(\hat{n}(\rho_s - \rho_w)\, g). \tag{3.16}$$

From (2.2), we find the scale $\hat{n}_i$ of porosity variation n_i' to be of the order

$$\hat{n}_2 \sim \hat{t}\hat{w}_2/\hat{b} \quad \text{and} \quad \hat{n}_i \sim \hat{t}\,\Delta\hat{w}_i/\hat{b} \quad (i = 1, 3), \tag{3.17}$$

hence

$$\hat{n}_i/\hat{n}_2 = O(\delta^{\frac{1}{2}}). \tag{3.18}$$

It follows that the omitted buoyancy term is of the order

$$O((\rho_s-\rho_w)\,g\,\rho_w\,g\hat{s}/\hat{D}_2), \tag{3.19}$$

while the remaining terms in (2.10) are of the order

$$\rho_w\,g\,\partial s'/\partial z = O(\rho_w\,g\,\hat{s}/\hat{b}). \tag{3.20}$$

The ratio of (3.19) to (3.20) is of the magnitude

$$\frac{\rho_s-\rho_w}{\rho_w}\frac{\rho_w\,g\hat{b}}{\hat{D}_2} = O(\mathscr{S}_T). \tag{3.21}$$

For a thick layer of soft clay, $\mathscr{S}_T$ may be of order unity, hence the body force terms cannot always be neglected. In this paper, it is assumed that $\mathscr{S}_T = O(1)$ in the aquitard. From (3.14), $\mathscr{S}_T$ is also a measure of the ratio of the vertical settlement $\hat{w}\hat{t}$ to the drawdown in the layered system. Therefore, from the values of $\hat{D}_2$ and $\hat{b}$ of the aquitard, one may also estimate the order of magnitude of the vertical subsidence from a unit drawdown.

In the aquifers the corresponding storage coefficients are

$$\mathscr{S}_{T_i} = (\hat{D}_2/\hat{D}_i)\,\mathscr{S}_T = O(\delta^{\frac{1}{2}})\,\mathscr{S}_T \quad (i = 1, 3), \tag{3.22}$$

which is much smaller than $\mathscr{S}_T$ in the aquitard.

(*e*) *Solid stresses*

With the aid of Hooke's law (A 3), it is readily seen that

$$\hat{\sigma}_{2zz} \approx D_2\frac{\partial w_2'}{\partial z}\hat{t} \approx \hat{D}_2\frac{\hat{w}\hat{t}}{\hat{b}} = \hat{D}_2\frac{\mathscr{S}_T\,\hat{s}}{\hat{b}} \approx \rho_w\,g\hat{s} \tag{3.23}$$

and for all layers

$$\frac{\sigma_{rz}'}{\sigma_{zz}'} \approx G\left(\frac{\partial u'}{\partial z}+\frac{\partial w'}{\partial r}\right)\Big/ D\frac{\partial w'}{\partial z} \approx \frac{\hat{u}}{\hat{w}} = O(\delta^{\frac{1}{2}}), \tag{3.24}$$

where (3.14) and (3.6) have been used.

(*f*) *Water table displacement*

Ignoring capillary effects, the dynamic boundary condition at the water table requires that $p = 0$. In the linearized limit $s' = h'$ at $\bar{\Gamma}_H$. Therefore the scale of h' is $\hat{s}$ also.

For convenience, all scales are summarized in the second column of table 1. (Lagrangian variables R, Z, T to be introduced in §4, are also included.) An equivalent set of scales is listed in the third column for normalization purposes. Note that k_i, a_v and D_i are normalized by their depth averages in each layer. In subsequent sections, all variables and dimensional parameters will be normalized according to column 3 in table 1 below, unless otherwise stated. All normalized quantities are distinguished by overhead tildes.

4. Lagrangian coordinates

Because the vertical deformation in the aquitard is expected to be comparable with the layer thickness, the eulerian positions of the interfaces and the water table are unknown *a priori*. To circumvent this difficulty we follow Gibson *et al.* (1967) and

Table 1. *Orders of magnitude and normalization scales* ($i = 1, 2, 3$)

variable or parameter	order of magnitude	normalization scale
Q	$\hat{Q}$	$\hat{Q}$
s_i'	$\hat{s} = \hat{Q}/2\pi\hat{b}\hat{k}_1$	$\hat{b}$
h'	$\hat{s}$	$\hat{b}$
$\bar{\sigma}_{izz}, \sigma'_{izz}$	$\rho_w g\hat{s}$	$\rho_w g\hat{b}$
σ'_{irz}	$\delta^{\frac{1}{2}}\rho_w g\hat{s}$	$\delta^{\frac{1}{2}}\rho_w g\hat{b}$
τ'_{izz}	$\rho_w g\hat{s}$	$\rho_w g\hat{b}$
p'	$\rho_w g\hat{s}$	$\rho_w g\hat{b}$
w_i'	$\hat{w} = \hat{k}_2\hat{s}/\hat{b}$	$\hat{k}_2$
u_i'	$\hat{u} = \delta^{\frac{1}{2}}\hat{w}$	$\delta^{\frac{1}{2}}\hat{k}_2$
b'	$\mathscr{S}_T\tilde{s}$	$\hat{b}$
B_i, b_i	$\hat{b}$	$\hat{b}$
r, a, R	$\hat{r} = \hat{b}/\delta^{\frac{1}{2}}$	$\hat{b}/\delta^{\frac{1}{2}}$
z, Z	$\hat{b}$	$\hat{b}$
t, T	$\mathscr{S}_T\hat{b}/\hat{k}_2$	$\mathscr{S}_T\hat{b}/\hat{k}_2$
D_i	$\hat{D}_i$	$\hat{D}_i$
a_v	$\hat{a}_v$	$\hat{a}_v$
k_i	$\hat{k}_i$	$\hat{k}_i$

use lagrangian coordinates (R, Z) which stand for the initial radial and vertical coordinates of each solid particle. Since the time derivatives in lagrangian coordinates mean material derivatives in eulerian coordinates, we distinguish the lagrangian time by T. The following relations hold between the eulerian and lagrangian coordinates,

$$r(R, Z, T) = R + r'(R, Z, T); \quad z(R, Z, T) = Z + z'(R, Z, T), \tag{4.1}$$

where r' and z' denote the solid displacements from the initial position and T denotes time. Normalizing according to column 3 of table 1, we get

$$\tilde{r} = \tilde{R} + \delta\tilde{r}'(\tilde{R}, \tilde{Z}, \tilde{T}); \quad \tilde{z} = \tilde{Z} + \tilde{z}'(\tilde{R}, \tilde{Z}, \tilde{T}). \tag{4.2}$$

The jacobian of transformation is

$$J = \frac{\partial(r, z)}{\partial(R, Z)} = \frac{\partial\tilde{z}}{\partial\tilde{Z}} + O(\delta) = 1 + \frac{\partial\tilde{z}'}{\partial\tilde{Z}} + O(\delta). \tag{4.3}$$

Thus, owing to the assumed sharp contrast of permeabilities, the jacobian is essentially the vertical strain of the solid. It follows by combining this result and the exact law of mass conservation of the solid matrix,

$$(1 - n)\, J = 1 - \bar{n}, \tag{4.4}$$

that

$$J = 1 + \frac{\partial\tilde{z}'}{\partial\tilde{Z}} + O(\delta) = \frac{1 - \bar{n}}{1 - n} = \frac{1 + e}{1 + \bar{e}}. \tag{4.5}$$

The spatial derivatives of any function F with respect to eulerian and lagrangian coordinates are related, in physical variables, by

$$\frac{\partial F}{\partial r} = \frac{1}{J}\left(\frac{\partial z}{\partial Z}\frac{\partial F}{\partial R} - \frac{\partial z}{\partial R}\frac{\partial F}{\partial Z}\right), \quad \frac{\partial F}{\partial z} = \frac{1}{J}\left(-\frac{\partial r}{\partial Z}\frac{\partial F}{\partial R} + \frac{\partial r}{\partial R}\frac{\partial F}{\partial Z}\right). \tag{4.6}$$

After normalization according to column 3 in table 1, the preceding relations can be approximated by

$$\frac{\partial \tilde{F}}{\partial \tilde{r}} = \frac{\partial \tilde{F}}{\partial \tilde{R}} - \frac{\partial \tilde{z}'/\partial \tilde{R}}{\partial \tilde{z}/\partial \tilde{Z}} \frac{\partial \tilde{F}}{\partial \tilde{Z}} + O(\delta), \tag{4.7}$$

$$\frac{\partial \tilde{F}}{\partial \tilde{z}} = \frac{1}{\partial \tilde{z}/\partial \tilde{Z}} \frac{\partial \tilde{F}}{\partial \tilde{Z}} + O(\delta) = \frac{1-n}{1-\bar{n}} \frac{\partial \tilde{F}}{\partial \tilde{Z}} + O(\delta) = \frac{1+\bar{e}}{1+e} \frac{\partial \tilde{F}}{\partial \tilde{Z}} + O(\delta). \tag{4.8}$$

Equation (4.8) will be repeatedly used in subsequent sections. If a function $\tilde{F}$ is defined on an initially horizontal surface composed of the same solid particles, e.g. the interfaces between two soil layers or the ground surface, the lagrangian coordinate $\tilde{Z}$ is fixed and $\partial \tilde{F}/\partial \tilde{Z} = 0$, hence

$$\partial \tilde{F}/\partial \tilde{r} = (\partial \tilde{F}/\partial \tilde{R})(1 + O(\delta)). \tag{4.9}$$

Note that the water table moves through the solid matrix, therefore (4.9) does not hold. Also the material time derivative is related to eulerian derivatives by

$$\frac{\partial \tilde{F}}{\partial \tilde{T}} = \frac{\partial \tilde{F}}{\partial \tilde{t}} + \delta \tilde{u}' \frac{\partial \tilde{F}}{\partial \tilde{r}} + \tilde{w}' \frac{\partial \tilde{F}}{\partial \tilde{z}} = \frac{\partial \tilde{F}}{\partial \tilde{t}} + \tilde{w}' \frac{\partial \tilde{F}}{\partial \tilde{z}} (1 + O(\delta)), \tag{4.10}$$

where $\tilde{u}'$ and $\tilde{w}'$ denote the $\tilde{r}$ and $\tilde{z}$ components of the solid velocity $\tilde{\boldsymbol{v}}_s'$.

We remark that the change from eulerian to lagrangian coordinates has a subtle effect on $\tilde{s}'$ defined in (2.5) in eulerian form. Evaluating the definition (2.5) at $\tilde{T} = 0$ and any $\tilde{T} \neq 0$ respectively, we get

$$0 = \tilde{p}(\tilde{r}(\tilde{R}, \tilde{Z}, 0), \tilde{z}(\tilde{R}, \tilde{Z}, 0), 0) + \tilde{Z} - \tilde{H} \tag{4.11a}$$

and

$$\tilde{s}'(\tilde{r}(\tilde{R}, \tilde{Z}, \tilde{T}), \tilde{z}(\tilde{R}, \tilde{Z}, \tilde{T}), \tilde{T}) = \tilde{p}(\tilde{r}(\tilde{R}, \tilde{Z}, \tilde{T}), \tilde{z}(\tilde{R}, \tilde{Z}, \tilde{T}), \tilde{T}) + \tilde{z}' + \tilde{Z} - \tilde{H}. \tag{4.11b}$$

Since $\tilde{p}(\tilde{r}(\tilde{R}, \tilde{Z}, 0), \tilde{z}(\tilde{R}, \tilde{Z}, 0), 0) = \tilde{\bar{p}}(\tilde{Z})$, the difference of (4.11*a*) and (4.11*b*) gives

$$\tilde{s}'(\tilde{r}(\tilde{R}, \tilde{Z}, \tilde{T}), \tilde{z}(\tilde{R}, \tilde{Z}, \tilde{T}), \tilde{T}) = \tilde{p}'(\tilde{r}(\tilde{R}, \tilde{Z}, \tilde{T}), \tilde{z}(\tilde{R}, \tilde{Z}, \tilde{T}), \tilde{T}) + \tilde{z}', \tag{4.12a}$$

which can be expressed simply as

$$\tilde{s}'(\tilde{R}, \tilde{Z}, \tilde{T}) = \tilde{p}'(\tilde{R}, \tilde{Z}, \tilde{T}) + \tilde{z}'. \tag{4.12b}$$

This result holds for a moving solid particle. In contrast, the corresponding relation for a fixed eulerian point is given by the last of (2.14).

5. The aquitard

In eulerian form, the z component of the exact equation of solid equilibrium reads

$$\frac{\partial \sigma_{2zz}}{\partial z} + \frac{1}{r} \frac{\partial}{\partial r}(r \sigma_{2rz}) = \rho_w g \frac{\partial s_2}{\partial z} + (1 - n_2)(\rho_s - \rho_w) g, \tag{5.1}$$

where σ_{2ij} is the sum of geostatic and perturbation stresses. After normalizing (5.1) according to the third column of table 1, we get

$$\frac{\partial \tilde{\sigma}_{2zz}}{\partial \tilde{z}} + \delta \frac{1}{\tilde{r}} \frac{\partial}{\partial \tilde{r}}(\tilde{r} \tilde{\sigma}_{2rz}) = \frac{\partial \tilde{s}_2'}{\partial \tilde{z}} + (1 - n_2)\left(\frac{\rho_s}{\rho_w} - 1\right). \tag{5.2}$$

The storage equation (2.7) in eulerian coordinates is similarly normalized to give

$$\frac{\partial}{\partial\tilde{z}}\left(\tilde{k}_2\frac{\partial\tilde{s}_2'}{\partial\tilde{z}}\right)+\delta\frac{1}{\tilde{r}}\frac{\partial}{\partial\tilde{r}}\left(\tilde{r}\tilde{k}_2\frac{\partial\tilde{s}_2'}{\partial\tilde{r}}\right)=\frac{\partial\tilde{w}_2'}{\partial\tilde{z}}+\delta\frac{1}{\tilde{r}}\frac{\partial}{\partial\tilde{r}}(\tilde{r}\tilde{u}_2'). \tag{5.3}$$

Let us introduce the following perturbation expansions for pumping-induced disturbances,

$$\left.\begin{aligned}\tilde{\sigma}'_{2zz}&=\tilde{\sigma}^{(0)}_{2zz}+\delta\tilde{\sigma}^{(1)}_{2zz}+\ldots, & \tilde{\sigma}'_{2rz}&=\tilde{\sigma}^{(0)}_{2rz}+\delta\tilde{\sigma}^{(1)}_{2rz}+\ldots,\\ \tilde{s}_2'&=\tilde{s}_2^{(0)}+\delta\tilde{s}_2^{(1)}+\ldots, & \tilde{w}_2'&=\tilde{w}_2^{(0)}+\delta w_2^{(1)}+\ldots,\\ \tilde{u}_2'&=\tilde{u}_2^{(0)}+\delta\tilde{u}_2^{(1)}+\ldots.\end{aligned}\right\} \tag{5.4}$$

By virtue of (4.8), (5.2) may be written in dimensionless lagrangian coordinates

$$\frac{\partial\tilde{\sigma}_2}{\partial\tilde{Z}}=\frac{\partial(\tilde{\bar{\sigma}}_2+\tilde{\sigma}_2^{(0)})}{\partial\tilde{Z}}=\frac{\partial\tilde{s}_2^{(0)}}{\partial\tilde{Z}}+(1-\bar{n}_2)\left(\frac{\rho_s}{\rho_w}-1\right)+O(\delta). \tag{5.5}$$

From here on we denote $\tilde{\sigma}^{(0)}_{2zz}$ simply by $\tilde{\sigma}_2^{(0)}$ for brevity. At $\tilde{T}=\tilde{t}=0$, $\tilde{z}=\tilde{Z}$, $\tilde{\sigma}_2^{(0)}=\tilde{s}_2^{(0)}=0$ and (5.5) describes the initial state $\tilde{\bar{\sigma}}_2$,

$$\partial\tilde{\bar{\sigma}}_2/\partial\tilde{Z}=(1-\bar{n}_2)(\rho_s/\rho_w-1). \tag{5.6}$$

The difference of (5.5) and (5.6) is

$$\partial\tilde{\sigma}_2^{(0)}/\partial\tilde{Z}=\partial\tilde{s}_2^{(0)}/\partial\tilde{Z}+O(\delta). \tag{5.7}$$

After using (5.4) and (4.8) the storage equation (5.3) also becomes

$$\frac{\partial}{\partial\tilde{Z}}\left(\tilde{k}_2\frac{1+\bar{e}_2}{1+e_2}\frac{\partial\tilde{s}_2^{(0)}}{\partial\tilde{Z}}\right)=\frac{\partial\tilde{w}_2^{(0)}}{\partial\tilde{Z}}+O(\delta). \tag{5.8}$$

The right-hand side can be further reduced to

$$\begin{aligned}\frac{\partial\tilde{w}_2^{(0)}}{\partial\tilde{Z}}&=\frac{\partial}{\partial\tilde{Z}}\frac{\partial(\tilde{Z}+\tilde{z}^{(0)})}{\partial\tilde{T}}=\frac{\partial}{\partial\tilde{T}}\frac{\partial(\tilde{Z}+\tilde{z}')}{\partial\tilde{Z}}=\frac{\partial}{\partial\tilde{T}}\left(\frac{1+e_2}{1+\bar{e}_2}\right)\\ &=\frac{1}{1+\bar{e}_2}\frac{\partial e_2}{\partial\tilde{T}}=\frac{1}{1+\bar{e}_2}\frac{\mathrm{d}e_2}{\mathrm{d}\tilde{\sigma}_2}\frac{\partial\tilde{\sigma}_2^{(0)}}{\partial\tilde{T}}=\frac{\tilde{a}_v}{1+\bar{e}_2}\frac{\partial\tilde{\sigma}_2^{(0)}}{\partial\tilde{T}},\end{aligned} \tag{5.9}$$

where (2.16) has been used. Combining (5.7), (5.8) and (5.9) we get

$$\frac{\partial}{\partial\tilde{Z}}\left(\tilde{k}_2\frac{1+\bar{e}_2}{1+e_2}\frac{\partial\tilde{\sigma}_2^{(0)}}{\partial\tilde{Z}}\right)=\frac{\tilde{a}_v}{1+\bar{e}_2}\frac{\partial\tilde{\sigma}_2^{(0)}}{\partial\tilde{T}}+O(\delta). \tag{5.10}$$

Equation (5.10) without the error term was first deduced by Gibson *et al.* (1967) for strictly one-dimensional consolidation of a soft layer without phreatic surface. It is obtained without omitting self weight or assuming constant total stress, unlike Cooper (1966) or Smiles & Rosenthal (1968). Based on §3 it is shown here to hold approximately for a three-dimensional problem in a shallow layer, with an $O(\delta)$ error. If $\tilde{Z}$ is replaced by $\tilde{X}$ defined according to

$$\frac{\mathrm{d}\tilde{X}}{\mathrm{d}\tilde{Z}}=\frac{1}{1+\bar{e}_2}\quad\text{or}\quad\tilde{X}=\tilde{B}_1+\int_{\tilde{B}_1}^{\tilde{Z}}\frac{\mathrm{d}\tilde{Z}}{1+\bar{e}_2}, \tag{5.11}$$

where $\tilde{B}_1$ is the normalized initial depth of the artesian aquifer, then (5.10) becomes

$$\frac{\partial}{\partial \tilde{X}}\left(\frac{\tilde{k}_2}{1+e_2}\frac{\partial \tilde{\sigma}_2^{(0)}}{\partial \tilde{X}}\right) = \tilde{a}_v \frac{\partial \tilde{\sigma}_2^{(0)}}{\partial \tilde{T}} + O(\delta). \tag{5.12}$$

It was shown by Gibson *et al.* that, by means of the constitutive law (2.16) or (2.17), (5.10) may also be expressed as a nonlinear partial differential equation for e,

$$\frac{\partial}{\partial \tilde{X}}\left(\frac{\tilde{k}_2}{1+e_2}\frac{\mathrm{d}\sigma_2^{(0)}}{\mathrm{d}e_2}\frac{\partial e_2}{\partial \tilde{X}}\right) - \left(\frac{\rho_s}{\rho_w}-1\right)\frac{\mathrm{d}}{\mathrm{d}e_2}\left(\frac{\tilde{k}_2}{1+e_2}\right)\frac{\partial e_2}{\partial \tilde{X}} = \frac{\partial e_2}{\partial \tilde{T}} + O(\delta). \tag{5.13}$$

They have pointed out that, by assuming

$$\frac{\tilde{k}_2}{1+e_2}\frac{\mathrm{d}\sigma_2^{(0)}}{\mathrm{d}e_2} \quad \text{and} \quad \frac{\mathrm{d}}{\mathrm{d}e_2}\left(\frac{\mathrm{d}e_2}{\mathrm{d}\sigma_2^{(0)}}\right)$$

to be constants, (5.13) can be reduced to a partial differential equation with constant coefficients. In our study more realistic features of the soil are explored, and no such simplifying assumptions will be made. However, the coordinate defined by (5.11) will have some numerical advantages and will be retained. Also in §8 we transform (5.10) and (5.12) for the drawdown $\tilde{s}_2^{(0)}$ in terms of which the boundary conditions on the interfaces are easier to state, as is deduced in later sections.

6. The artesian aquifer

Again based on the normalization scales in table 1, the dimensionless form of the storage equation (2.7) is

$$\frac{\partial}{\partial \tilde{z}}\left(\tilde{k}_1\frac{\partial \tilde{s}_1'}{\partial \tilde{z}}\right) + \frac{\delta}{\tilde{r}}\frac{\partial}{\partial \tilde{r}}\left(r\tilde{k}_1\frac{\partial \tilde{s}_1'}{\partial \tilde{r}}\right) = \frac{\delta^2}{\tilde{r}}\frac{\partial(\tilde{r}\tilde{u}_1')}{\partial \tilde{r}} + \delta^{\frac{3}{2}}\frac{\partial \tilde{w}_1'}{\partial \tilde{z}}. \tag{6.1}$$

The boundary condition on the impermeable bedrock is

$$\partial \tilde{s}_1'/\partial \tilde{z} = 0. \tag{6.2}$$

On the lower interface $\Gamma_1 : \tilde{z} = \tilde{b}_1(\tilde{r}, \tilde{t})$, the normal flux must be continuous. The exact expression of the upward unit normal vector is, in physical and dimensionless forms,

$$\boldsymbol{n}_1 = \frac{\boldsymbol{e}_z - (\partial b_1'/\partial r)\,\boldsymbol{e}_r}{[1+(\partial b_1'/\partial r)^2]^{\frac{1}{2}}} = \frac{\boldsymbol{e}_z - \delta(\partial \tilde{b}_1'/\partial \tilde{r})\,\boldsymbol{e}_r}{[1+\delta^2(\partial \tilde{b}_1'/\partial \tilde{r})^2]^{\frac{1}{2}}}, \tag{6.3}$$

which can be approximated by

$$\boldsymbol{n}_1 = O(\delta)\,\boldsymbol{e}_r + [1+O(\delta^2)]\,\boldsymbol{e}_z. \tag{6.4}$$

Since $\hat{k}_2/\hat{k}_1 = O(\delta)$, (2.23) can be normalized to

$$\tilde{k}_1\left(\delta^{\frac{1}{2}}\frac{\partial \tilde{s}_1'}{\partial \tilde{r}}\boldsymbol{e}_r + \frac{\partial \tilde{s}_1'}{\partial \tilde{z}}\boldsymbol{e}_z\right)\cdot \boldsymbol{n}_1 = \delta \tilde{k}_2\left(\delta^{\frac{1}{2}}\frac{\partial \tilde{s}_2'}{\partial \tilde{r}}\boldsymbol{e}_r + \frac{\partial \tilde{s}_2'}{\partial \tilde{z}}\boldsymbol{e}_z\right)\cdot \boldsymbol{n}_1, \tag{6.5a}$$

or

$$\delta \tilde{k}_2\,\partial \tilde{s}_2'/\partial \tilde{z} = \tilde{k}_1\,\partial \tilde{s}_1'/\partial \tilde{z} + O(\delta^{\frac{3}{2}}) \quad \text{on } \Gamma_1. \tag{6.5b}$$

This condition is applied at the instantaneous position of $\Gamma_1(\tilde{r}, \tilde{t})$.

Introducing the perturbation expansion

$$\tilde{s}_1' = \tilde{s}_1^{(0)} + \delta \tilde{s}_1^{(1)} + O(\delta^{\frac{3}{2}}), \tag{6.6}$$

we can readily show from (6.1), (6.2) and (6.5b) that to order $O(\delta^0)$, $\tilde{s}_1^{(0)}$ is constant in depth,

$$\tilde{s}_1^{(0)} = \tilde{s}_1^{(0)}(\tilde{r}, \tilde{t}) = \tilde{s}_2^{(0)}(\tilde{r}, \tilde{b}_1, \tilde{t}). \tag{6.7}$$

The second equality follows by continuity of pressure. Thus the flow in the artesian aquifer is primarily horizontal. At the next order $O(\delta)$ we have

$$\frac{\partial}{\partial \tilde{z}}\left(\tilde{k}_1 \frac{\partial \tilde{s}_1^{(1)}}{\partial \tilde{z}}\right) = -\frac{1}{\tilde{r}}\frac{\partial}{\partial \tilde{r}}\left(\tilde{r}\tilde{k}_1 \frac{\partial \tilde{s}_1^{(0)}}{\partial \tilde{r}}\right) = -\frac{1}{\tilde{r}}\left[\frac{\partial}{\partial \tilde{r}}\left(\tilde{r}\tilde{k}_1 \frac{\partial \tilde{s}_2^{(0)}}{\partial \tilde{r}}\right)\right]_{\Gamma_1} \tag{6.8}$$

with the boundary conditions

$$\partial \tilde{s}_1^{(1)}/\partial \tilde{z} = 0 \quad (\tilde{z} = 0), \tag{6.9}$$

$$\tilde{k}_1 \partial \tilde{s}_1^{(1)}/\partial \tilde{z} = \tilde{k}_2 \partial \tilde{s}_2^{(0)}/\partial \tilde{z} \quad (\tilde{z} = \tilde{b}_1(\tilde{r}, \tilde{t})). \tag{6.10}$$

The ordinary differential equation (6.8) and the boundary conditions (6.9) and (6.10) define an inhomogeneous boundary value problem for $\tilde{s}_1^{(1)}$ in $\tilde{z} \in [0, \tilde{b}_1]$. Integration once, we get

$$\tilde{k}_2 \frac{\partial \tilde{s}_2^{(0)}}{\partial \tilde{z}} = -\frac{\tilde{b}_1}{\tilde{r}}\frac{\partial}{\partial \tilde{r}}\left(\tilde{r}\tilde{k}_1 \frac{\partial \tilde{s}_2^{(0)}}{\partial \tilde{r}}\right) \quad \text{on } \Gamma_1. \tag{6.11}$$

Mathematically this is the *solvability condition* for $\tilde{s}_1^{(1)}$, since the homogeneous boundary value problem admits the non-trivial solution $\tilde{s}_1^{(0)}$. Equation (6.11) serves as a boundary condition for the aquitard drawdown $\tilde{s}_2^{(0)}$.

Let us transform (6.11) to lagrangian coordinates according to (4.8) and (4.9). Since the aquifer is hard, $e_1 = \bar{e}_1$ so that $\tilde{k}_1 \approx \bar{\tilde{k}}_1$ with an error at $O(\delta^{\frac{1}{2}})$, the hydraulic conductivity $\tilde{k}_1$ can be taken outside the parenthesis. Also $\tilde{b}_1 = \tilde{B}_1 + O(\delta^{\frac{1}{2}})$ from (3.12). Equation (6.11) can therefore be transformed to

$$\tilde{k}_2\left(\frac{1+\bar{e}_2}{1+e_2}\right)\frac{\partial \tilde{s}_2^{(0)}}{\partial \tilde{Z}} = -\frac{\bar{\tilde{k}}_1 \tilde{B}_1}{\tilde{R}}\frac{\partial}{\partial \tilde{R}}\left(\tilde{R}\frac{\partial \tilde{s}_2^{(0)}}{\partial \tilde{R}}\right) \quad \text{on } \bar{\Gamma}_1, \tag{6.12}$$

where (4.8) has been used and $\bar{\Gamma}_1$ denotes Γ_1 at $\tilde{T} = 0$. Note that this boundary condition contains a second-order derivative of $\tilde{s}_2^{(0)}$ with respect to the radial lagrangian coordinate $\tilde{R}$. From (2.31), we obtain after normalization

$$\tilde{R}\,\partial \tilde{s}_2^{(0)}/\partial \tilde{R} = \nu \tilde{Q}(\tilde{T}) \quad \tilde{R} = \tilde{a}, \quad \text{on } \bar{\Gamma}_1, \tag{6.13}$$

where $\tilde{Q} = Q/\hat{Q}$ and the dimensionless parameter ν is defined to be

$$\nu = \hat{s}/\hat{b} = \hat{Q}/2\pi \hat{b}^2 \hat{k}_1, \tag{6.14}$$

which is a measure of the well discharge. We further require

$$\tilde{s}_2^{(0)} \to 0 \quad \text{as} \quad \tilde{R} \to \infty, \quad \text{on } \Gamma_1. \tag{6.15}$$

Since the approximate equations are derived for $\tilde{R} = O(\hat{r})$, the solution is valid for all $\tilde{R} > \tilde{a}$ only if the well radius $\tilde{a}$ is of the same order as $\hat{r}$, i.e. $\tilde{a} = a/\hat{r} = O(1)$. If $a \ll \hat{b}$, a uniformly valid theory would require a fully three-dimensional *inner* problem near the well where both radial and vertical length scales are comparable. The inner solution should then be matched to the *outer* solution to (6.11). This is a prohibitively complicated task. In later examples we choose a small value of $\hat{a}$ which is still much larger than the typical layer depth.

7. The phreatic aquifer

Because the water table can move through the solid matrix significantly, the fluid mechanics in this layer is highly nonlinear. Our plan in this section is as follows. We first examine the storage equation in the water layer and the boundary conditions on the interface Γ_2 and the water table Γ_H. From order $O(\delta)$ we get a solvability condition for $\tilde{s}_3^{(1)}$, leading to a boundary condition for $\tilde{s}_2^{(0)}$ on Γ_2. Considerable effort is then given to manipulate this condition which involves nonlinear coefficients depending on $\tilde{\sigma}_2^{(0)}$ and e_2.

In the instantaneous wet zone, $\tilde{b}_1+\tilde{b}_2<\tilde{z}<\tilde{h}$, the dimensionless eulerian storage equation is similar to (6.1), hence,

$$\frac{\partial}{\partial\tilde{z}}\left(\tilde{k}_3\frac{\partial\tilde{s}_3'}{\partial\tilde{z}}\right)+\frac{\delta}{\tilde{r}}\frac{\partial}{\partial\tilde{r}}\left(\tilde{r}\tilde{k}_3\frac{\partial\tilde{s}_3'}{\partial\tilde{r}}\right)=O(\delta^{\frac{3}{2}}). \tag{7.1}$$

Let us normalize the kinematic boundary condition (2.28) on the water table,

$$-\delta\frac{\kappa}{\mathscr{S}_T}\frac{\partial\tilde{h}'}{\partial\tilde{t}}+\delta\frac{\tilde{k}_3}{n_3}\frac{\partial\tilde{s}_3'}{\partial\tilde{r}}\frac{\partial\tilde{h}'}{\partial\tilde{r}}-\delta^2\kappa\tilde{u}_3'\frac{\partial\tilde{h}'}{\partial\tilde{r}}-\frac{\tilde{k}_3}{n_3}\frac{\partial\tilde{s}_3'}{\partial\tilde{z}}+\delta\kappa\tilde{w}_3'=0\quad\text{on }\Gamma_H, \tag{7.2}$$

where

$$\kappa\equiv\hat{k}_1/\hat{k}_3. \tag{7.3}$$

As for the flux condition on the interface Γ_2, we begin by finding the upward unit normal vector:

$$\begin{aligned}\boldsymbol{n}_2&=\frac{\boldsymbol{e}_z-(\partial b_2'/\partial r)\,\boldsymbol{e}_r}{[1+(\partial b_2'/\partial r)^2]^{\frac{1}{2}}}=\frac{\boldsymbol{e}_z-\delta^{\frac{1}{2}}(\partial\tilde{b}_2'/\partial\tilde{r})\,\boldsymbol{e}_r}{[1+\delta(\partial\tilde{b}_2'/\partial\tilde{r})^2]^{\frac{1}{2}}}\\&=\left[1-\tfrac{1}{2}\delta\left(\frac{\partial\tilde{b}_2'}{\partial\tilde{r}}\right)^2\right]\boldsymbol{e}_z-\delta^{\frac{1}{2}}\frac{\partial\tilde{b}_2'}{\partial\tilde{r}}\boldsymbol{e}_r+O(\delta^{\frac{3}{2}}),\end{aligned} \tag{7.4}$$

which is quite different from the unit normal to Γ_1 because Γ_2 is deformed by $O(\hat{b})$. The flux condition (2.23) is normalized to

$$\delta\kappa\tilde{k}_2\left(\delta^{\frac{1}{2}}\frac{\partial\tilde{s}_2'}{\partial\tilde{r}}\boldsymbol{e}_r+\frac{\partial\tilde{s}_2'}{\partial\tilde{z}}\boldsymbol{e}_z\right)\cdot\boldsymbol{n}_2=\tilde{k}_3\left(\delta^{\frac{1}{2}}\frac{\partial\tilde{s}_3'}{\partial\tilde{r}}\boldsymbol{e}_r+\frac{\partial\tilde{s}_3'}{\partial\tilde{z}}\boldsymbol{e}_z\right)\cdot\boldsymbol{n}_2. \tag{7.5}$$

Keeping terms up to $O(\delta)$ we have

$$-\delta\kappa\tilde{k}_2\frac{\partial\tilde{s}_2'}{\partial\tilde{z}}=\delta\tilde{k}_3\frac{\partial\tilde{s}_3'}{\partial\tilde{r}}\frac{\partial\tilde{b}_2'}{\partial\tilde{r}}-\tilde{k}_3\frac{\partial\tilde{s}_3'}{\partial\tilde{z}}\left[1-\tfrac{1}{2}\delta\left(\frac{\partial\tilde{b}_2'}{\partial\tilde{r}}\right)^2\right]+O(\delta^2)\quad\text{on }\Gamma_2. \tag{7.6}$$

Let us now introduce the perturbation expansions to solve the boundary value problem defined by (7.1), (7.2) and (7.6):

$$\begin{gathered}\tilde{s}_3'=\tilde{s}_3^{(0)}+\delta\tilde{s}_3^{(1)}+\ldots,\quad\tilde{w}_3'=\tilde{w}_3^{(0)}+\delta\tilde{w}_3^{(1)}+\ldots,\\\tilde{h}'=\tilde{h}^{(0)}+\delta\tilde{h}^{(1)}+\ldots.\end{gathered} \tag{7.7}$$

At the leading order $O(\delta^0)$, it is evident from (7.1), (7.2) and (7.6) that $\tilde{s}_3^{(0)}$ is also independent of depth so that

$$\tilde{s}_3^{(0)}=\tilde{s}_3^{(0)}(\tilde{r},\tilde{t})=\tilde{h}^{(0)},\quad\tilde{b}_1+\tilde{b}_2<\tilde{z}<\tilde{h}. \tag{7.8}$$

The last equality follows from (2.25) at order $O(\delta^0)$.

At order $O(\delta)$ we have from (7.1)

$$\frac{\partial}{\partial\tilde{z}}\left(\tilde{k}_3\frac{\partial\tilde{s}_3^{(1)}}{\partial\tilde{z}}\right)=-\frac{1}{\tilde{r}}\frac{\partial}{\partial\tilde{r}}\left(\tilde{r}\tilde{k}_3\frac{\partial\tilde{s}_3^{(0)}}{\partial\tilde{r}}\right)\quad(\tilde{b}_1+\tilde{b}_2)<\tilde{z}<\tilde{h}, \tag{7.9}$$

while the boundary conditions (7.6) and (7.2) give respectively

$$\tilde{k}_3\frac{\partial\tilde{s}_3^{(1)}}{\partial\tilde{z}}=\kappa\tilde{k}_2\frac{\partial\tilde{s}_2^{(0)}}{\partial\tilde{z}}+\tilde{k}_3\frac{\partial\tilde{s}_3^{(0)}}{\partial\tilde{r}}\frac{\partial\tilde{b}_2'}{\partial\tilde{r}}+\tilde{k}_3\frac{\partial\tilde{s}_3^{(0)}}{\partial\tilde{z}}\left(\frac{\partial\tilde{b}_2'}{\partial\tilde{r}}\right)^2\quad\text{on }\Gamma_2 \tag{7.10}$$

and

$$\frac{\tilde{k}_3}{n_3}\frac{\partial\tilde{s}_3^{(1)}}{\partial\tilde{z}}=-\frac{\kappa}{\mathscr{S}_T}\frac{\partial\tilde{h}^{(0)}}{\partial\tilde{t}}+\frac{\tilde{k}_3}{n_3}\frac{\partial\tilde{s}_3^{(0)}}{\partial\tilde{r}}\frac{\partial\tilde{h}^{(0)}}{\partial\tilde{r}}+\kappa\tilde{w}_3^{(0)}\quad\text{on }\Gamma_H. \tag{7.11}$$

Note that in (7.9) to (7.11) $\tilde{s}_3^{(0)}$ can be replaced by $\tilde{s}_2^{(0)}$ (Γ_2) by virtue of the continuity of pressure, and that the last term in (7.10) vanishes because of (7.8). Now we proceed to derive a solvability condition for $\tilde{s}_3^{(1)}$. Integrating (7.9) in $\tilde{z}$ across the wet zone in the top layer we obtain

$$\left[\tilde{k}_3\frac{\partial\tilde{s}_3^{(1)}}{\partial\tilde{z}}\right]_{\Gamma_H}-\left[\tilde{k}_3\frac{\partial\tilde{s}_3^{(1)}}{\partial\tilde{z}}\right]_{\Gamma_2}=-(\tilde{H}+\tilde{h}^{(0)}-\tilde{b}_1-\tilde{b}_2)\frac{1}{\tilde{r}}\left[\frac{\partial}{\partial\tilde{r}}\left(\tilde{r}\tilde{k}_3\frac{\partial\tilde{s}_3^{(0)}}{\partial\tilde{r}}\right)\right]_{\Gamma_2}. \tag{7.12}$$

Use of (7.10) and (7.11) in (7.12) leads to

$$-n_3\frac{\kappa}{\mathscr{S}_T}\frac{\partial\tilde{h}^{(0)}}{\partial\tilde{t}}+\tilde{k}_3\frac{\partial\tilde{s}_3^{(0)}}{\partial\tilde{r}}\frac{\partial\tilde{h}^{(0)}}{\partial\tilde{r}}+n_3\kappa\tilde{w}_3^{(0)}$$

$$-\kappa\left[\tilde{k}_2\frac{\partial\tilde{s}_2^{(0)}}{\partial\tilde{z}}\right]_{\Gamma_2}-\tilde{k}_3\frac{\partial\tilde{s}_3^{(0)}}{\partial\tilde{r}}\frac{\partial\tilde{b}_2'}{\partial\tilde{r}}=-[\tilde{H}+\tilde{h}^{(0)}-\tilde{b}_1-\tilde{b}_2]\frac{1}{\tilde{r}}\frac{\partial}{\partial\tilde{r}}\left(\tilde{r}\tilde{k}_3\frac{\partial\tilde{s}_3^{(0)}}{\partial\tilde{r}}\right). \tag{7.13}$$

This is the solvability condition.

Now let us apply the dynamic boundary condition $\tilde{s}_3^{(0)}=\tilde{h}^{(0)}=\tilde{s}_2^{(0)}(\Gamma_2)$ to rewrite (7.13)

$$n_3\kappa\tilde{w}_3^{(0)}-n_3\frac{\kappa}{\mathscr{S}_T}\frac{\partial\tilde{h}^{(0)}}{\partial\tilde{t}}-\kappa\left[\tilde{k}_2\frac{\partial\tilde{s}_2^{(0)}}{\partial\tilde{z}}\right]_{\Gamma_2}+\tilde{k}_3\left[\frac{\partial\tilde{s}_2^{(0)}}{\partial\tilde{r}}\right]_{\Gamma_2}\frac{\partial}{\partial\tilde{r}}(\tilde{s}_3^{(0)}-\tilde{b}_2')$$

$$+(\tilde{H}+\tilde{h}^{(0)}-\tilde{b}_1-\tilde{b}_2)\left[\frac{1}{\tilde{r}}\frac{\partial}{\partial\tilde{r}}\left(\tilde{r}\tilde{k}_3\frac{\partial s_2^{(0)}}{\partial\tilde{r}}\right)\right]_{\Gamma_2}=0, \tag{7.14}$$

where $\tilde{s}_2^{(0)}$ is evaluated at the instantaneous interface $\Gamma_2:\tilde{z}=\tilde{b}_2(\tilde{r},\tilde{t})$. To eliminate $\tilde{w}_3^{(0)}=\tilde{w}_2^{(0)}(\Gamma_2)$ we integrate the storage equation (2.7) at leading order across the entire aquitard, and use the boundary condition (6.10)

$$\tilde{w}_2^{(0)}(\Gamma_2)=\left[\tilde{k}_2\frac{\partial\tilde{s}_2^{(0)}}{\partial\tilde{z}}\right]_{\Gamma_1}^{\Gamma_2}=\left[\tilde{k}_2\frac{\partial\tilde{s}_2^{(0)}}{\partial\tilde{z}}\right]_{\Gamma_2}+\tilde{b}_1\left[\frac{1}{\tilde{r}}\frac{\partial}{\partial\tilde{r}}\left(\tilde{r}\tilde{k}_1\frac{\partial\tilde{s}_2^{(0)}}{\partial\tilde{r}}\right)\right]_{\Gamma_1}. \tag{7.15}$$

We now change the factor $\tilde{H}+\tilde{h}^{(0)}-\tilde{b}_1-\tilde{b}_2$ into a more convenient form. At $\tilde{t}=\tilde{T}=0$, the interface Γ_2 is at $\tilde{z}=\tilde{B}_1+\tilde{B}_2$ while the water table is at $\tilde{z}=\tilde{H}$. At any later time $\tilde{t}$, Γ_2 is at $\tilde{z}=\tilde{B}_1+\tilde{B}_2+\tilde{b}_2'$, while Γ_H is at $\tilde{z}=\tilde{H}+\tilde{h}'$. The net change of thickness of the wet zone in the top aquifer is approximately equal to the net rise of the water

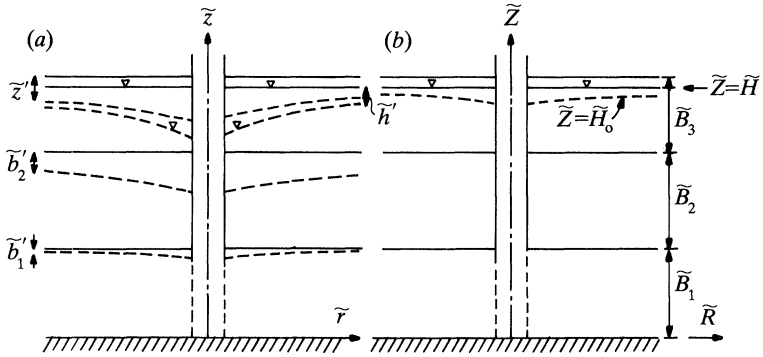

Figure 1. Definition sketch (*a*) in eulerian coordinates; (*b*) in lagrangian coordinates.

table relative to the ground surface, $\tilde{h}'-\tilde{b}_2'+O(\delta^{\frac{1}{2}})$; the error being due to the small compaction of the two aquifers (cf. (3.11)). Note that the solid particles coinciding with the current water table at any $\tilde{t}$ come originally from the level $\tilde{z}=\tilde{H}_0$ which is not the same as $\tilde{H}$ and varies with time and horizontal position, as sketched in figure 1. Clearly, the following equality holds,

$$\tilde{H}_0-\tilde{H}=\tilde{h}'-\tilde{b}_2'+O(\delta^{\frac{1}{2}}). \tag{7.16}$$

It follows that

$$\begin{aligned}\tilde{H}+\tilde{h}^{(0)}-\tilde{b}_1-\tilde{b}_2&=\tilde{H}+\tilde{H}_0-\tilde{H}+\tilde{b}_2'-\tilde{B}_1-\tilde{B}_2-\tilde{b}_2'+O(\delta^{\frac{1}{2}})\\&=\tilde{H}-\tilde{B}_1-\tilde{B}_2-(\tilde{H}-\tilde{H}_0)+O(\delta^{\frac{1}{2}}).\end{aligned} \tag{7.17}$$

Making use of (7.15) and (7.17), (7.14) can be rewritten as

$$\begin{aligned}(1-n_3)\kappa\left[\tilde{k}_2\frac{\partial\tilde{s}_2^{(0)}}{\partial\tilde{z}}\right]_{\Gamma_2}&=-n_3\frac{\kappa}{\mathscr{S}_T}\frac{\partial\tilde{h}^{(0)}}{\partial\tilde{t}}+\frac{n_3\tilde{b}_1\kappa}{\tilde{r}}\left[\frac{\partial}{\partial\tilde{r}}\left(\tilde{r}\tilde{k}_1\frac{\partial\tilde{s}_2^{(0)}}{\partial\tilde{r}}\right)\right]_{\Gamma_1}+\tilde{k}_3\left[\frac{\partial\tilde{s}_2^{(0)}}{\partial\tilde{r}}\right]_{\Gamma_2}\\&\times\frac{\partial}{\partial\tilde{r}}(\tilde{s}_3^{(0)}-\tilde{b}_2')+(\tilde{H}-\tilde{B}_1-\tilde{B}_2-(\tilde{H}-\tilde{H}_0))\frac{1}{\tilde{r}}\left[\frac{\partial}{\partial\tilde{r}}\left(\tilde{r}\tilde{k}_3\frac{\partial\tilde{s}_2^{(0)}}{\partial\tilde{r}}\right)\right]_{\Gamma_2}.\end{aligned} \tag{7.18}$$

Changing (7.18) from eulerian to lagrangian coordinates according to (4.8), (4.9) and (4.10), using $\tilde{h}^{(0)}=\tilde{s}_2^{(0)}(\bar{\Gamma}_2)$, and the fact that the phreatic aquifer is hard, we obtain

$$\begin{aligned}(1-\bar{n}_3)\kappa\left(\tilde{k}_2\frac{1+\bar{e}_2}{1+e_2}\frac{\partial\tilde{s}_2^{(0)}}{\partial\tilde{Z}}\right)_{\bar{\Gamma}_2}&=-\bar{n}_3\frac{\kappa}{\mathscr{S}_T}\left[\frac{\partial\tilde{s}_2^{(0)}}{\partial\tilde{T}}\right]_{\bar{\Gamma}_2}+\bar{n}_3\kappa\tilde{B}_1\tilde{\tilde{k}}_1\frac{1}{\tilde{R}}\frac{\partial}{\partial\tilde{R}}\left(\tilde{R}\frac{\partial\tilde{s}_2^{(0)}}{\partial\tilde{R}}\right)_{\bar{\Gamma}_1}\\&+\tilde{\tilde{k}}_3\left[\frac{\partial\tilde{s}_2^{(0)}}{\partial\tilde{R}}\right]_{\bar{\Gamma}_2}\frac{\partial}{\partial\tilde{R}}(\tilde{s}_3^{(0)}-\tilde{b}_2')+[(\tilde{H}-\tilde{B}_1-\tilde{B}_2)-(\tilde{H}-\tilde{H}_0)]\frac{\tilde{\tilde{k}}_3}{\tilde{R}}\left[\frac{\partial}{\partial\tilde{R}}\left(\tilde{R}\frac{\partial\tilde{s}_2^{(0)}}{\partial\tilde{R}}\right)\right]_{\bar{\Gamma}_2}.\end{aligned} \tag{7.19}$$

The negligible compaction in the aquifers has been used in replacing n_3 by $\bar{n}_3$ and $\tilde{k}_1$ by $\tilde{\tilde{k}}_1$.

As a last step we note first from (7.16) that

$$\tilde{s}_3^{(0)}-\tilde{b}_2'=\tilde{h}^{(0)}-\tilde{b}_2'=\tilde{H}_0-\tilde{H}+O(\delta^{\frac{1}{2}}). \tag{7.20}$$

Furthermore it is shown in Appendix B that

$$\tilde{\sigma}_2^{(0)}(\bar{\Gamma}_2)=-(1-\bar{n}_3)(\tilde{H}-\tilde{H}_0)=(1-\bar{n}_3)(\tilde{s}_3^{(0)}-\tilde{b}_2'). \tag{7.21}$$

By combining (7.19) and (7.21) we obtain finally,

$$\frac{1-\bar{n}_3}{\bar{n}_3}\kappa\left(\tilde{k}_2\frac{1+\bar{e}_2}{1+e_2}\frac{\partial\tilde{s}_2^{(0)}}{\partial\tilde{Z}}\right)_{\bar{\Gamma}_2}=-\frac{\kappa}{\mathscr{S}_T}\left[\frac{\partial\tilde{s}_2^{(0)}}{\partial\tilde{T}}\right]_{\bar{\Gamma}_2}+\kappa\tilde{B}_1\tilde{\tilde{k}}_1\frac{1}{\tilde{R}}\frac{\partial}{\partial\tilde{R}}\left(\tilde{R}\frac{\partial\tilde{s}_2^{(0)}}{\partial\tilde{R}}\right)_{\bar{\Gamma}_1}$$
$$+(\tilde{H}-\tilde{B}_1-\tilde{B}_2)\frac{\tilde{\tilde{k}}_3}{\bar{n}_3}\frac{1}{\tilde{R}}\frac{\partial}{\partial\tilde{R}}\left(\tilde{R}\frac{\partial\tilde{s}_2^{(0)}}{\partial\tilde{R}}\right)_{\bar{\Gamma}_2}+\frac{\tilde{\tilde{k}}_3}{\bar{n}_3(1-\bar{n}_3)}$$
$$\times\left[\frac{\partial\tilde{\sigma}_2^{(0)}}{\partial\tilde{R}}\frac{\partial\tilde{s}_2^{(0)}}{\partial\tilde{R}}+\tilde{\sigma}_2^{(0)}\frac{1}{\tilde{R}}\frac{\partial}{\partial\tilde{R}}\left(\tilde{R}\frac{\partial\tilde{s}_2^{(0)}}{\partial\tilde{R}}\right)\right]_{\bar{\Gamma}_2}. \tag{7.22}$$

The preceding equation serves as a boundary condition on $\bar{\Gamma}_2$ for $\tilde{s}_2^{(0)}$ in the aquitard. Note that the finite displacement of the water table contributes to the nonlinear terms in the last brackets. In addition nonlinearity arises from e_2 which depends on $\tilde{\sigma}_2$ through the empirical law (2.17). Hence water and the soil matrix are strongly coupled. The unusual mathematical features of (7.22) are two-fold. (i) It involves $\tilde{s}_2^{(0)}$ on both $\bar{\Gamma}_1$ and $\bar{\Gamma}_2$. (ii) It involves both time and radial derivatives of $\tilde{s}_2^{(0)}$ and implies radial diffusion. Therefore we need the following boundary conditions

$$\partial\tilde{s}_2^{(0)}/\partial\tilde{R}=0 \quad \tilde{R}=\tilde{a} \quad \text{on } \bar{\Gamma}_2, \tag{7.23}$$

$$\tilde{s}_2^{(0)}\to 0, \quad \tilde{R}\to\infty \quad \text{on } \bar{\Gamma}_2, \tag{7.24}$$

and the initial condition

$$\tilde{s}_2^{(0)}(\tilde{R},\tilde{Z},0)=0, \quad \tilde{T}=0. \tag{7.25}$$

8. Equation governing the aquitard drawdown

Since the boundary conditions (6.12) and (7.22) are expressed for $\tilde{s}_2^{(0)}$, it is convenient to express the governing equation (5.10) in terms of the aquitard drawdown also. Integrating the lagrangian equation (5.7) with respect to $\tilde{Z}$ we get

$$\tilde{\sigma}_2^{(0)}=\tilde{\sigma}_2^{(0)}(\bar{\Gamma}_2)+[\tilde{s}_2^{(0)}-\tilde{s}_2^{(0)}(\bar{\Gamma}_2)], \tag{8.1}$$

where $\tilde{\sigma}_2^{(0)}$ denotes the stress at any $\tilde{Z}$. Taking the lagrangian time derivative of (8.1), i.e. by following $\bar{\Gamma}_2$, we obtain

$$\frac{\partial\tilde{\sigma}_2^{(0)}}{\partial\tilde{T}}=\frac{\partial\tilde{\sigma}_2^{(0)}(\bar{\Gamma}_2)}{\partial\tilde{T}}+\left(\frac{\partial\tilde{s}_2^{(0)}}{\partial\tilde{T}}-\frac{\partial\tilde{s}_2^{(0)}(\bar{\Gamma}_2)}{\partial\tilde{T}}\right). \tag{8.2}$$

Since $\partial\tilde{b}_2'/\partial\tilde{T}=\mathscr{S}_T\tilde{w}_2$, the lagrangian time derivative of (7.21) is

$$(1-\bar{n}_3)(\partial\tilde{s}_3^{(0)}/\partial\tilde{T}-\mathscr{S}_T\tilde{w}_3^{(0)})=\partial\tilde{\sigma}_2^{(0)}(\bar{\Gamma}_2)/\partial\tilde{T}. \tag{8.3}$$

It then follows from (8.2) that

$$\frac{\partial\tilde{\sigma}_2^{(0)}}{\partial\tilde{T}}=(1-\bar{n}_3)\left[\frac{\partial\tilde{s}_2^{(0)}(\bar{\Gamma}_2)}{\partial\tilde{T}}-\mathscr{S}_T\tilde{w}_2^{(0)}(\bar{\Gamma}_2)\right]+\frac{\partial\tilde{s}_2^{(0)}}{\partial\tilde{T}}-\frac{\partial\tilde{s}_2^{(0)}(\bar{\Gamma}_2)}{\partial\tilde{T}}$$
$$=-\bar{n}_3\frac{\partial\tilde{s}_2^{(0)}(\bar{\Gamma}_2)}{\partial\tilde{T}}-(1-\bar{n}_3)\mathscr{S}_T\tilde{w}_2^{(0)}(\bar{\Gamma}_2)+\frac{\partial\tilde{s}_2^{(0)}}{\partial\tilde{T}}=-\bar{n}_3\frac{\partial\tilde{s}_2^{(0)}(\bar{\Gamma}_2)}{\partial\tilde{T}}+\frac{\partial\tilde{s}_2^{(0)}}{\partial\tilde{T}}$$
$$-(1-\bar{n}_3)\mathscr{S}_T\left[\tilde{k}_2\frac{1+\bar{e}_2}{1+e_2}\frac{\partial\tilde{s}_2^{(0)}}{\partial\tilde{Z}}\right]_{\bar{\Gamma}_1}^{\bar{\Gamma}_2}, \quad \tilde{B}_1<\tilde{Z}<\tilde{B}_1+\tilde{B}_2. \tag{8.4}$$

The last equation is obtained with the help of (7.15). This transforms the right-hand side of (5.10) from $\tilde{\sigma}_2^{(0)}$ to $\tilde{s}_2^{(0)}$. The left-hand side of (5.10) is easily rewritten by using (5.7), yielding,

$$\frac{\partial \tilde{s}_2^{(0)}}{\partial \tilde{T}} = \bar{n}_3 \frac{\partial \tilde{s}_2^{(0)}(\bar{\Gamma}_2)}{\partial \tilde{T}} + (1-\bar{n}_3)\,\mathscr{S}_T\left[\tilde{k}_2 \frac{1+\bar{e}_2}{1+e_2}\frac{\partial \tilde{s}_2^{(0)}}{\partial \tilde{Z}}\right]_{\bar{\Gamma}_1}^{\bar{\Gamma}_2} + \frac{1+\bar{e}_2}{\tilde{a}_v}\frac{\partial}{\partial \tilde{Z}}\left(\tilde{k}_2 \frac{1+\bar{e}_2}{1+e_2}\frac{\partial \tilde{s}_2^{(0)}}{\partial \tilde{Z}}\right), \quad \tilde{B}_1 < \tilde{Z} < \tilde{B}_1 + \tilde{B}_2. \tag{8.5}$$

An expression for $\partial \tilde{s}_2^{(0)}(\bar{\Gamma}_2)/\partial \tilde{T}$ can be obtained by evaluating (8.5) on $\bar{\Gamma}_2$. The result can be substituted into (8.5) to yield finally

$$\frac{\partial \tilde{s}_2^{(0)}}{\partial \tilde{T}} = \frac{1+\bar{e}_2}{\tilde{a}_v}\frac{\partial}{\partial \tilde{Z}}\left(\tilde{k}_2 \frac{1+\bar{e}_2}{1+e_2}\frac{\partial \tilde{s}_2^{(0)}}{\partial \tilde{Z}}\right) + \mathscr{S}_T\left[\tilde{k}_2 \frac{1+\bar{e}_2}{1+e_2}\frac{\partial \tilde{s}_2^{(0)}}{\partial \tilde{Z}}\right]_{\bar{\Gamma}_1}^{\bar{\Gamma}_2} + \bar{e}_3\left(\frac{1+\bar{e}_2}{\tilde{a}_v}\right)_{\bar{\Gamma}_2}\left[\frac{\partial}{\partial \tilde{Z}}\left(\tilde{k}_2 \frac{1+\bar{e}_2}{1+e_2}\frac{\partial \tilde{s}_2^{(0)}}{\partial \tilde{Z}}\right)\right]_{\bar{\Gamma}_2}, \quad \tilde{B}_1 < \tilde{Z} < \tilde{B}_1 + \tilde{B}_2. \tag{8.6}$$

In summary, (8.6) is the governing equation for the vertical diffusion of $\tilde{s}_2^{(0)}$ in the aquitard. At any fixed $\tilde{R}$, (6.12) and (7.22) provide two boundary conditions on the bounding interfaces $\bar{\Gamma}_1$ and $\bar{\Gamma}_2$. On the other hand, the same two interface conditions govern the radial variation of $\tilde{s}_2^{(0)}$. Together with two radial boundary conditions (6.13) and (6.15) on $\bar{\Gamma}_1$, two radial boundary conditions (7.23) and (7.24) on $\bar{\Gamma}_2$, and the initial condition (7.25), we have now defined an initial-boundary value problem for $\tilde{s}_2^{(0)}$. The mathematical problem involves two space dimensions and time, and can be solved by an alternating direction scheme.

9. Other physical quantities

In the aquitard, $\tilde{s}_2^{(0)}$, e_2, $\tilde{k}_2$, and $\tilde{a}_v$ are related by constitutive laws and are calculated along with $\tilde{s}_2^{(0)}$ at each time step, as will be described in §11. Once they are determined, the water table displacement relative to the instantaneous ground surface follows from (7.21):

$$\tilde{H} - \tilde{H}_0 = -(\tilde{h}^{(0)} - \tilde{b}_2') + O(\delta^{\frac{1}{2}}) = -\tilde{\sigma}_2^{(0)}(\bar{\Gamma}_2)/(1-\bar{n}_3). \tag{9.1}$$

From the coordinate relation (4.2), the transform relation (4.5) and the smallness of the aquifer compaction, the aquitard settlement is given by

$$\tilde{b}_2' = \tilde{z}'(\bar{\Gamma}_2) = \tilde{z}'(\bar{\Gamma}_3) + O(\delta^{\frac{1}{2}}) = \int_{\tilde{B}_1}^{\tilde{B}_2} \frac{\partial \tilde{z}'}{\partial \tilde{Z}}\,\mathrm{d}\tilde{Z} = \int_{\tilde{B}_1}^{\tilde{B}_2} \frac{e_2 - \bar{e}_2}{1+\bar{e}_2}\,\mathrm{d}\tilde{Z}. \tag{9.2}$$

Physically, the integrand in (9.2) is the ratio of the change of void volume to the initial volume in a soil column of unit cross section. Thus the aquitard compaction is due to the total void change throughout the depth.

To obtain the change of the total stress $\tilde{\tau}_2'$ we need the lagrangian form of (2.8) for solid equilibrium in the vertical direction

$$\frac{\partial(\tilde{\tau} + \tilde{\tau}_2')}{\partial \tilde{Z}} = \left[(1-\bar{n}_2)\frac{\rho_s}{\rho_w} + \frac{1-\bar{n}_2}{1-n_2}n_2\right]. \tag{9.3}$$

In the initial state, (9.3) is

$$\partial\tilde{\bar{\tau}}_2/\partial\tilde{Z} = [(1-\bar{n}_2)\rho_s/\rho_w + \bar{n}_2]. \tag{9.4}$$

Integrating the difference of (9.3) and (9.4) we get

$$\tilde{\tau}'_2 = \tilde{\tau}'_2(\bar{\Gamma}_2) - \int_{\tilde{z}}^{\tilde{B}_2} \frac{e_2-\bar{e}_2}{1+e_2}\,\mathrm{d}\tilde{Z} \tag{9.5}$$

throughout the aquitard. Thus the total stress is in general not constant in depth and the variation is caused by the accumulated change of void ratio in the aquitard.

The effective stress perturbation is given by (8.1). For alternate expressions to be used later we apply (7.20) and (9.1) on the upper interface $\bar{\Gamma}_2$

$$\tilde{s}_2^{(0)}(\bar{\Gamma}_2) = -(\tilde{H}-\tilde{H}_0)+\tilde{b}'_2 = \tilde{\sigma}_2^{(0)}(\bar{\Gamma}_2)/(1-\bar{n}_3)+\tilde{b}'_2. \tag{9.6}$$

It then follows from (8.1) and (9.2) that

$$\tilde{\sigma}_2^{(0)} + \bar{e}_3\,\tilde{\sigma}_2^{(0)}(\bar{\Gamma}_2) = \tilde{s}_2^{(0)} - \int_{\tilde{B}_1}^{\tilde{B}_2} \frac{e_2-\bar{e}_2}{1+\bar{e}_2}\,\mathrm{d}\tilde{Z} = \tilde{s}_2^{(0)} - \int_{\tilde{X}_1}^{\tilde{X}} (e_2-\bar{e}_2)\,\mathrm{d}\tilde{X}. \tag{9.7}$$

10. The limiting case of a hard aquitard

Hantush (1960) studied a three-layered soil system where $\hat{D}_1, \hat{D}_2, \hat{D}_3$ are comparable, yet all large so that $\mathscr{S}_T = \rho_w g\hat{b}/\hat{D}_2$ is small. If $\mathscr{S}_T \ll 1$ is assumed in our theory, the limit should check with Hantush's theory with $\hat{D}_1, \hat{D}_3 \gg \hat{D}_2$.

By definition (2.19) a_v is small for large $\hat{D}_2$. It follows from (2.16) that $\mathrm{d}e_2/\mathrm{d}\sigma_{2zz} \ll 1$ so that the deformation in the aquitard is small, i.e. $e_2(z) \approx$ const. $= \bar{e}_2(\bar{\Gamma}_2)$ and $\tilde{k}_2 \approx \tilde{\bar{k}} \approx 1$. Also $J \approx \partial z/\partial Z \approx 1$ so that the difference between eulerian and lagrangian coordinates becomes negligible. At the upper interface $\bar{\Gamma}_2$, as $\mathscr{S}_T \to 0$, we obtain from (7.22)

$$\partial\tilde{s}_2^{(0)}/\partial\tilde{T} \to 0 \quad \text{on } \bar{\Gamma}_2. \tag{10.1}$$

Equation (8.5) then reduces to a simple diffusion equation in eulerian coordinates

$$\frac{\partial\tilde{s}_2^{(0)}}{\partial\tilde{t}} = \tilde{D}_2\frac{\partial}{\partial\tilde{z}}\left(\tilde{k}_2\frac{\partial\tilde{s}_2^{(0)}}{\partial\tilde{z}}\right), \tag{10.2}$$

where

$$\tilde{D}_2 = (1+e_2)/\tilde{a}_v. \tag{10.3}$$

The boundary condition (6.12) on the lower interface $\bar{\Gamma}_1$ becomes

$$\tilde{k}_2\frac{\partial\tilde{s}_2^{(0)}}{\partial\tilde{z}} = -\tilde{\bar{k}}_1\tilde{b}\frac{1}{\tilde{r}}\frac{\partial}{\partial\tilde{r}}\left(\tilde{r}\frac{\partial\tilde{s}_2^{(0)}}{\partial\tilde{r}}\right) \quad \text{on } \bar{\Gamma}_1. \tag{10.4}$$

At the upper interface, (10.1) and the initial condition (7.25) may be combined to give

$$\tilde{s}_2^{(0)} = 0 \quad \text{on } \bar{\Gamma}_2. \tag{10.5}$$

Equations (10.2) to (10.5) indeed agree with Hantush in the limit of $\hat{D}_1, \hat{D}_3 \gg \hat{D}_2$.

For constant $\tilde{k}_2$ this special problem can be solved formally by integral transforms, from which asymptotic solutions for large and small time have been used to verify the numerical scheme to be sketched in §11, which is similar to that used in Fallou *et al.* (1991).

11. Numerical scheme

As the vertical variation of drawdown $\tilde{s}_2^{(0)}$ is expected to be more pronounced near the lower rather than the upper interface, non-uniform discretization along the $\tilde{Z}$ axis would be needed for numerical efficiency. Since the coordinate $\tilde{X}$ introduced by (5.11) is related to an integral of $\bar{e}_2$, a more convenient uniform grid in $\tilde{X}$ can be used to achieve same or better accuracy, with the same number of nodes. In our computations, transformation from $\tilde{Z}$ to $\tilde{X}$ is made. Since radial variations are also more rapid near the well of a small radius, the radial coordinate is transformed by

$$\eta = \ln \tilde{R}/\tilde{a} \tag{11.1}$$

so that

$$\tilde{R}\frac{\partial \tilde{s}_2^{(0)}}{\partial \tilde{R}} \to \frac{\partial \tilde{s}_2^{(0)}}{\partial \eta} \quad \text{and} \quad \frac{1}{\tilde{R}}\frac{\partial}{\partial \tilde{R}}\left(\tilde{R}\frac{\partial \tilde{s}_2^{(0)}}{\partial \tilde{R}}\right) \to \frac{1}{\tilde{R}^2}\frac{\partial^2 \tilde{s}_2^{(0)}}{\partial \eta^2}. \tag{11.2}$$

The computational domain is the large but finite rectangle $0 = \eta_1 < \eta < \eta_N$, $\tilde{X}_1 < \tilde{X} < \tilde{X}_M$ discretized into $(N-1)\times(M-1)$ small rectangles with $N-1$ uniform intervals in η and $M-1$ uniform intervals in $\tilde{X}$. At each grid point and the nth time step $\tilde{s}_2^{(0)}$ is denoted by s_{ij}^n with $i = 1, \ldots, N$ and $j = 1, \ldots, M$. Suppose that all quantities are known everywhere at $n\Delta\tilde{T}$. The procedure for advancing to $(n+1)\,\Delta\tilde{T}$ is as follows.

(*a*) *Interior points*

For all interior points along the same vertical line we use the Euler forward scheme to solve the vertical diffusion equation (8.6) and march to the next time step, hence obtain s_{ij}^{n+1}, for $j = 2, 3, \ldots, M-1$. This is repeated N times for N vertical lines.

(*b*) *Interface points*

Step 1. For grid points along the interfaces several iterations are needed to advance to $(n+1)\,\Delta\tilde{T}$, since the boundary condition (7.22) on $\bar{\Gamma}_2$ is nonlinear. We first choose values of e_2, $\tilde{k}_2$, $\tilde{a}_v$ and $\tilde{\sigma}_2^{(0)}$ and the nth time step as the first trial values ${}^0e_{ij}^{n+1}$, ${}^0k_{ij}^{n+1}$, ${}^0(a_v)_{ij}^{n+1}$ and ${}^0\sigma_{ij}^{n+1}$. On the lower interface $\bar{\Gamma}_1$, we use central differences to solve the 2-point boundary value problem in the radial direction defined by the ordinary differential equation (6.12) with (6.13) and (6.15). On the upper interface, the radial diffusion equation (7.22) is solved with (7.23) and (7.24) by Crank–Nicholson scheme. The first iterates ${}^1s_{i,1}^{n+1}$ and ${}^1s_{i,M}^{n+1}$ are then found.

Step 2. We then calculate the second iterate ${}^2\sigma_{ij}^{n+1}$ from (9.7) by using the first iterate in the right-hand side, etc.

Step 3. At the kth iteration of the stress, we recalculate e_2 according to the two-coefficient model constitutive law described in §2*b*. During the initial stage of pumping, the aquitard undergoes virgin compression; $\tilde{\sigma}'$ is negative (compression) and increases in magnitude with time. Therefore the larger value for virgin compression must be taken for C_c. During reduced pumping or recharging $\tilde{\sigma}'$ changes sign at $\tilde{\sigma}' = \tilde{\sigma}'_c$, and becomes positive. The small swelling index C'_c must replace C_c. The same C'_c is used during recompression until $\tilde{\sigma}'$ returns to $\tilde{\sigma}'_c$. Further increase in compression beyond $\tilde{\sigma}'_c$, C_c must be used again. In this way ${}^ke_{ij}^{n+1}$ and ${}^ka_{vij}^{n+1}$ are obtained. Kozeny's formula is then used to get ${}^kk_{ij}^{n+1}$; ${}^ks_{i,1}^{n+1}$ and ${}^ks_{i,M}^{n+1}$ are recalculated by repeating Step 1. The iteration process is continued until satisfactory convergence is achieved in $\tilde{\sigma}_2^{(0)}$ and $\tilde{s}_2^{(0)}$ at all grid points. The criterion for convergence is set to be

$$|{}^{k+1}\sigma_{ij}^{n+1} - {}^k\sigma_{ij}^{n+1}|/|{}^k\sigma_{ij}^{n+1}| < 10^{-6}. \tag{11.3}$$

The number of iterations required is usually less than 10 for early times ($\tilde{T} < 0.2$) and less than 5 otherwise.

The solution procedure is now complete up to $(n+1)$th time step, and the same procedure is repeated for the next time step.

The consistency of the finite difference approximations is kept at $O(\Delta\eta)^2$, $O(\Delta\tilde{X})^2$, and $O(\Delta\tilde{T})$. Several values of η_N, $\Delta\tilde{X}$ and $\Delta\eta$ have been tested to ensure convergence. It is found that by increasing η_N beyond 15 with fixed $\Delta\eta = 0.15$, no changes can be observed in the solution. Keeping $\eta_N = 15$, a few different $\Delta\eta$ values were used to see the accuracy of finite difference approximation. For example, the difference in $s^n_{1,1}$ for $\Delta\eta = 0.1$ was less than 0.1%. In all cases, we use $\Delta\eta = 0.15351$.

The vertical range of computation in $\tilde{X}$ varies with the initial void ratio distribution $\bar{e}_2$, which depends on $\mathscr{S}_T$. Now the total thickness in $\tilde{X}$ is

$$\tilde{X}_2 - \tilde{X}_1 = \int_{\tilde{B}_1}^{\tilde{B}_2} \frac{\mathrm{d}\tilde{Z}}{1+\bar{e}_2} \tag{11.4}$$

according to (5.11), which must be also affected by $\mathscr{S}_T$. For example, $\tilde{X}_2 - \tilde{X}_1 = 0.13$ for a soft aquitard with $\mathscr{S}_T = 0.45$ and $\bar{e}_2(\bar{\Gamma}_2) = 8.0$. Numerical tests show that convergence is reached when $\Delta\tilde{X} < 0.01$. In all cases, $\tilde{X}_2 - \tilde{X}_1$ is divided into 30 equal intervals.

The scheme is explicit in time and instabilities are possible when $\Delta\tilde{T}$ is greater than a certain value depending on $\Delta\tilde{X}$. The governing equation (8.6) is diffusive in $\tilde{X}$ with variable diffusion coefficient $\tilde{k}_2(1+\bar{e}_2)^2/\tilde{a}_v(1+e_2)$ which varies with time. By an approximate linear stability analysis, $\Delta\tilde{T}$ must be such that

$$\frac{\tilde{k}_2}{\tilde{a}_v}\frac{(1+\bar{e}_2)^2}{1+e_2}\frac{\Delta\tilde{T}}{(\Delta\tilde{X})^2} < O(1). \tag{11.5}$$

Typically $\Delta\tilde{T} = 0.0001$ is used for $\mathscr{S}_T < 0.6$ and $\Delta\tilde{T} = 5\times10^{-5}$ for $\mathscr{S}_T > 0.6$.

To check the numerical scheme, a simple problem was chosen with $e_2 = e_0 =$ constant, $\tilde{k}_2 = 1$ and $\mathscr{S}_T \ll 1$. The resulting problem is linear and can be solved analytically by Laplace transform, which has been used to confirm our numerical solution, as was done in Fallou *et al.* (1991).

12. Numerical results

In our numerical examples all three layers are assumed to be of equal thickness, hence the normalized depth is unity for all layers ($\tilde{B}_1 = \tilde{B}_2 = \tilde{B}_3 = 1$), and the two aquifers have the same hydraulic conductivity ($\kappa = \hat{k}_1/\hat{k}_3 = 1$) and compression index. The dimensionless well radius $\tilde{a}$ is taken to be $\tilde{a} = 0.05$ whose precise value is important only very near the well. At $\tilde{T} = 0$, the water table is at the mid-height of the top aquifer ($\tilde{H} - \tilde{B}_1 - \tilde{B}_2 = 0.5$).

(a) *Initial state*

The initial state of static equilibrium is a one-dimensional problem governed by (5.6). By using (2.15) and (2.17), it is reduced to a nonlinear first-order differential equation for $\bar{e}_2$ which can be numerically integrated for a prescribed $\bar{e}_2$ at the top of the layer. After $\bar{e}_2(\tilde{Z})$ is calculated $\tilde{\bar{k}}_2(\tilde{Z})$, $\tilde{\bar{\sigma}}_2(\tilde{Z})$ and $\tilde{\bar{D}}_2(\tilde{Z})$ follow from the constitutive

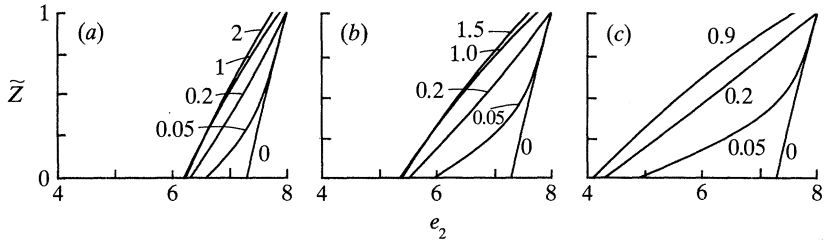

Figure 2. Vertical variation of the aquitard void ratio e_2 at $\tilde{R} = 0.5$ for various pumping rates: (*a*) $\nu = 0.5$, (*b*) $\nu = 1.0$, (*c*) $\nu = 2.0$. The numbers by each curve denote the dimensionless time $\tilde{T}$.

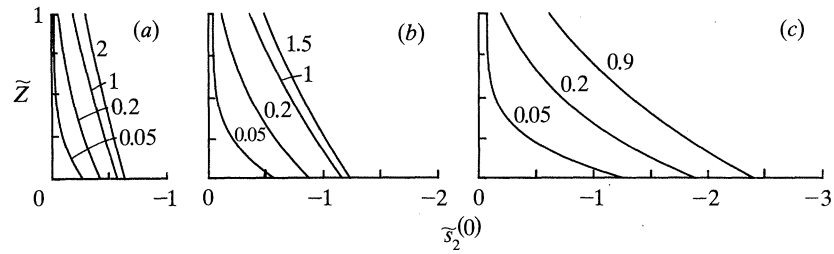

Figure 3. Depth and time variation of the aquitard drawdown $\tilde{s}_2^{(0)}$ at $\tilde{R} = 0.5$ for (*a*) $\nu = 0.5$, (*b*) $\nu = 1.0$, (*c*) $\nu = 2.0$.

laws. Details can be found in Fallou *et al.* (1991) for the same three-layered system. In this paper the following void ratios are chosen for an exceptionally soft and porous aquitard typical of Mexico City clay (for which the range of e is from 6 to 10 (Zeevaert 1983; Marsal 1957)):

$$\bar{e}_1(\bar{\Gamma}_1) = 2.0, \quad \bar{e}_2(\bar{\Gamma}_2) = 8.0, \quad \bar{e}_3(\bar{\Gamma}_3) = 2.5, \quad C_c = 6.0.$$

The storage coefficient $\mathscr{S}_T$ is then calculated to be $\mathscr{S}_T = 0.45$.

(*b*) *Steady pumping*

Three different rates of pumping are examined: $\nu = 0.5$, 1.0 and 2.0, labelled respectively in figure 2 by (*a*), (*b*) and (*c*).

(i) *Void ratio*

The vertical variation of the aquitard void ratio e_2 at $\tilde{R} = 0.5$ is plotted in figure 2*a–c*. As is expected of vertical diffusion (cf. (5.13)), the void ratio perturbation is first confined to the lower part of the aquitard and spreads in time over the entire depth. As a result of finite deformation, e_2 is reduced by a considerable amount from its initial value $\bar{e}_2$.

The vertical variations of hydraulic conductivity $\tilde{k}_2$ and the coefficient of compressibility $\tilde{a}_v$ at $\tilde{R} = 0.5$ are similar to those of e_2 and are omitted.

(ii) *Drawdown*

The vertical distribution of the aquitard drawdown at $\tilde{R} = 0.5$ is shown in figure 3*a–c*. Note that the magnitude of $\tilde{s}_2^{(0)}(\bar{\Gamma}_2)$ roughly increases in accordance with the increment of the pumping rate ν. Again the drawdown diffuses upwards from the lower interface and finally approaches a linear distribution in $\tilde{Z}$ for large time.

In figure 4, the drawdowns at the soil interfaces $\bar{\Gamma}_1$ and $\bar{\Gamma}_2$ are shown as functions

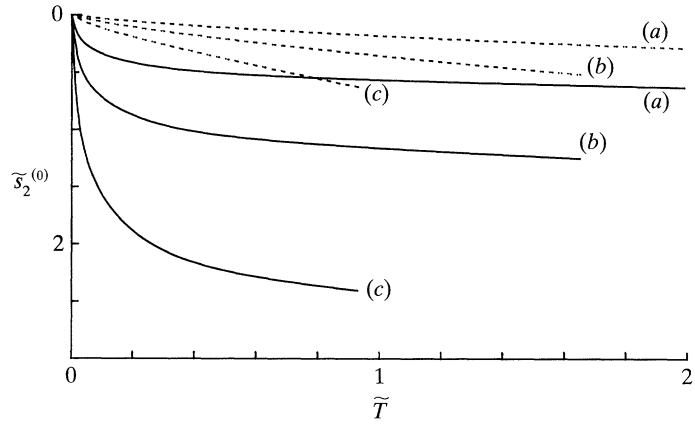

Figure 4. Time variation of the aquitard drawdowns on the interfaces $\tilde{s}_2^{(0)}(\Gamma_1)$ (solid) and $\tilde{s}_2^{(0)}(\bar{\Gamma}_2)$ (dashed) at $\tilde{R} = 0.2$: (*a*) $\nu = 0.5$, (*b*) $\nu = 1.0$ and (*c*) $\nu = 2.0$.

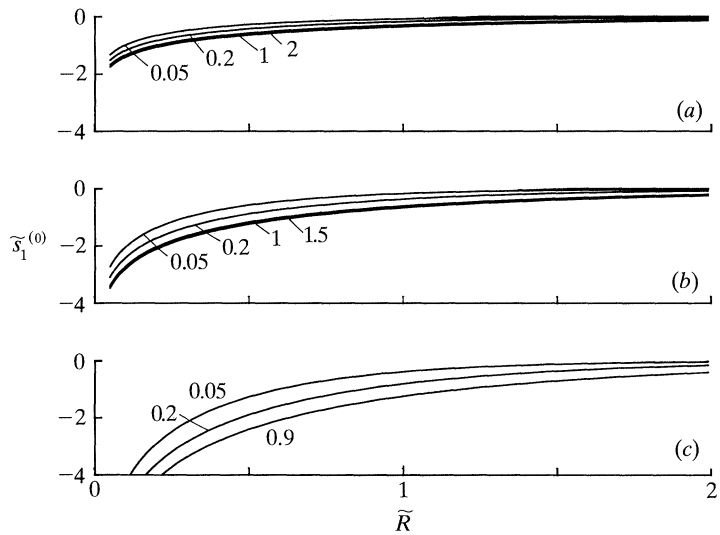

Figure 5. Radial variation of the drawdown in the artesian aquifer: (*a*) $\nu = 0.5$, (*b*) $\nu = 1.0$, (*c*) $\nu = 2.0$.

of time for $\tilde{R} = 0.5$. These are also the drawdowns in the aquifers because of continuity. Note that $\tilde{s}_2^{(0)}(\bar{\Gamma}_2)$ becomes comparable to the layer thickness as the pumping rate ν increases. For the higher pumping rates $\nu = 1.0$ and $\nu = 2.0$, computation has to be stopped at $\tilde{T} = 1.5$ and 1.0 respectively beyond which the water table sinks below the interface $\bar{\Gamma}_2$ into the aquitard (cf. figure 8); the present formulation must be further modified. Such an extension is not pursued here.

The radial variation of $\tilde{s}_2^{(0)}(\bar{\Gamma}_1)$ is shown in figure 5*a–c* and similarly that of $\tilde{s}_2^{(0)}(\bar{\Gamma}_2)$ in figure 6*a–c*. Obviously, near the well, $\tilde{s}_2^{(0)}(\bar{\Gamma}_1)$ varies with $\tilde{R}$ rapidly while $\tilde{s}_2^{(0)}(\bar{\Gamma}_2)$ varies slowly. Recall that the flow is essentially horizontal in the aquifers and vertical in the aquitard. This result implies that the large amount of water pumped out of the artesian aquifer is replenished only to a minor extent by the phreatic aquifer.

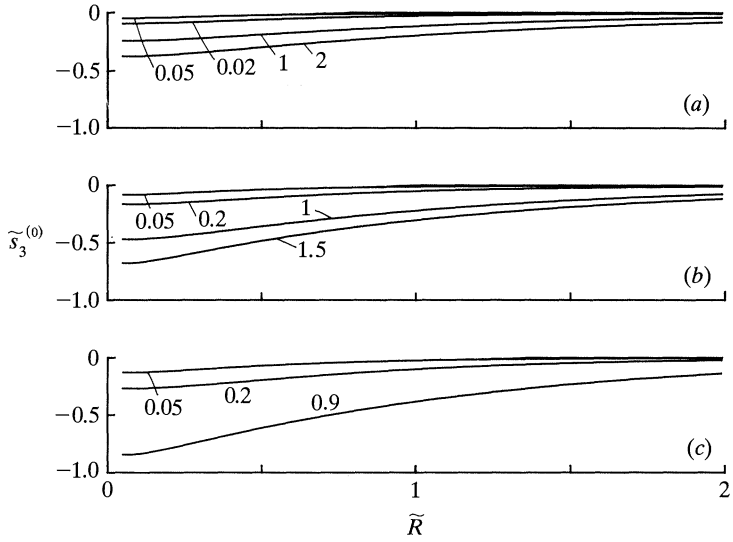

Figure 6. Radial variation of the drawdown in the phreatic aquifer for (*a*) $\nu = 0.5$, (*b*) $\nu = 1.0$, (*c*) $\nu = 2.0$.

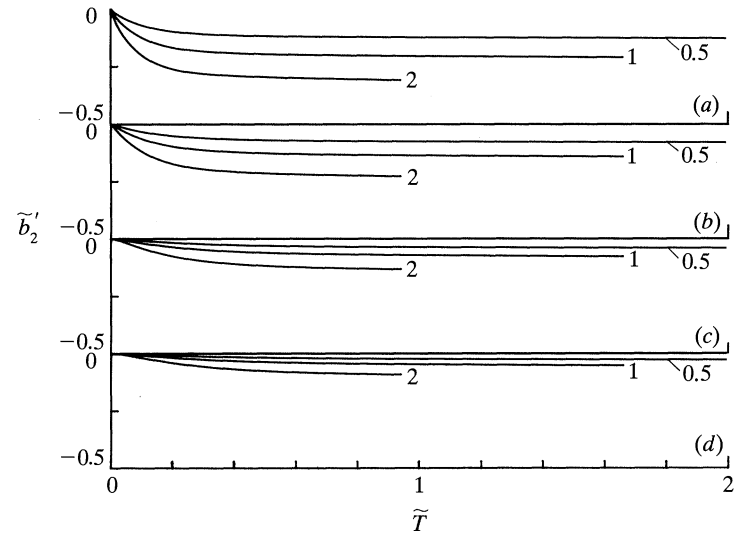

Figure 7. Time variation of normalized ground subsidence at (*a*) $\tilde{R} = 0.2$, (*b*) $\tilde{R} = 0.5$, (*c*) $\tilde{R} = 1.1$ and (*d*) $\tilde{R} = 1.5$ for various pumping rates $\nu = 0.5$, 1.0, 2.0.

(iii) *Ground subsidence*

The vertical subsidence is plotted in figure 7*a–d* as a function of time. Because of the radial diffusion, $\tilde{b}_2'$ reaches the steady state much sooner near the well. Note from (9.2) subsidence is caused by the accumulated changes of void ratio throughout the entire depth of the aquitard. Therefore its transition toward the final value is much more rapid than the local void ratio near the top of the layer; the latter decreases by the slow upward diffusion.

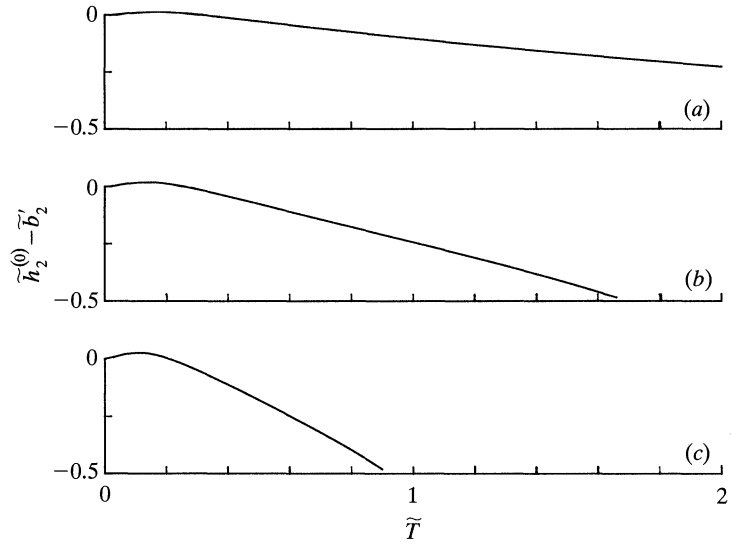

Figure 8. Time variation of the watertable displacement relative to ground surface, $\tilde{h}^{(0)} - \tilde{b}_2'$ at $\tilde{R} = 0.2$ for (*a*) $\nu = 0.5$, (*b*) $\nu = 1.0$, (*c*) $\nu = 2.0$.

(iv) *Water table*

Rather than the absolute vertical displacement, it is the vertical displacement of the water table relative to the current ground surface that is of practical interest. The latter is also the difference between the initial and the current depths of the water layer above the moving interface $\bar{\Gamma}_2$, i.e. $\tilde{h}^{(0)} - \tilde{b}_2' = \tilde{s}_2^{(0)}(\bar{\Gamma}_2) - \tilde{b}_2'$. By taking the difference of figures 6 and 7 one can obtain the plot of $\tilde{h}^{(0)} - \tilde{b}_2'$ against $\tilde{R}$ for a set of $\tilde{T}$. We show instead in figure 8*a–c* the time variation of $\tilde{h}^{(0)} - \tilde{b}_2'$ for $\tilde{R} = 0.2$. It can be seen that for small $\tilde{R}$, the depth $\tilde{h}^{(0)} - \tilde{b}_2'$ increases at first, then decreases for large $\tilde{T}$. This is a manifestation of the Mandel–Cryer effect (Mandel 1953; Cryer 1963; Gibson *et al.* 1989), known to occur in a related problem of pumping from an infinitely deep consolidating aquifer (Veruijt 1969). In the present case, deformation occurs mainly in the aquitard, but the physical mechanism is similar and can be explained as follows. Near the well and for small time, the effect of pumping in the artesian aquifer is not immediately felt at the upper interface $\bar{\Gamma}_2$ hence $\tilde{s}_2^{(0)}(\bar{\Gamma}_2)$ is relatively small, see figure 4. However, being affected by the variation of void ratio in the entire aquitard, the subsidence of the upper interface $\tilde{b}_2'$ responds to pumping much more quickly. As a consequence, $\tilde{h}^{(0)} - \tilde{b}_2'$ is positive for small $\tilde{T}$ near the well. As time increases, $\tilde{s}_2^{(0)}(\bar{\Gamma}_2)$ steadily increases and dominates over $\tilde{b}_2'$. This results in a steady decrease of $\tilde{h}^{(0)} - \tilde{b}_2'$ in figure 8. Thus the initial rise of water table near the well is due to the instantaneous compaction of the aquitard and the slow diffusion of the pore pressure.

The depth dependence of the effective stress perturbation $\tilde{\sigma}_2^{(0)}$ differs from that of $\tilde{s}_2^{(0)}$ only by the aquitard settlement on the upper interface, hence need not be plotted.

(v) *Total stress perturbation*

In figure 9*a–c*, the depth dependence of the total stress perturbation at $\tilde{R} = 0.5$ is shown for a set of $\tilde{T}$. Departure from uniformity is more noticeable for higher rate of pumping (and of course also for softer aquitard). Thus the common assumption of constant total stress is no longer accurate here. The non-uniformity is caused by

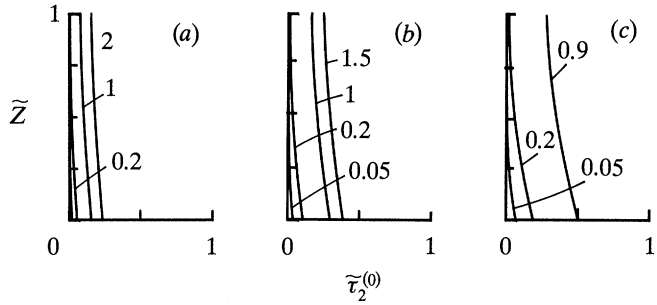

Figure 9. Vertical variation of normalized total stress perturbation $\tilde{\tau}_2^{(0)}$ at $\tilde{R} = 0.5$ for (*a*) $\nu = 0.5$, (*b*) $\nu = 1.0$, (*c*) $\nu = 2.0$.

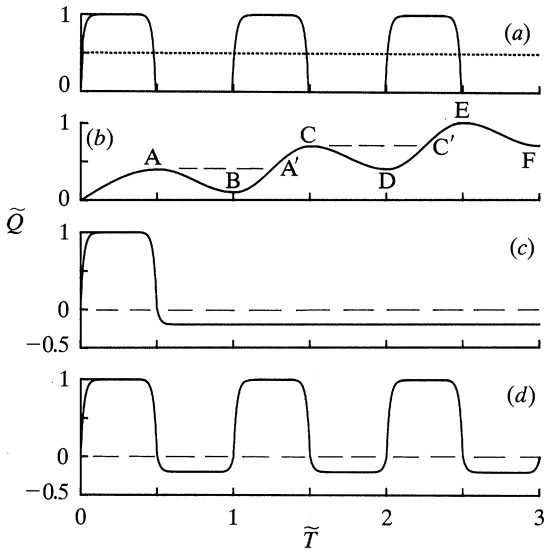

Figure 10. Transient pumping patterns.

aquitard compaction and gravity, represented by the integral term in (9.5). As time becomes large, compaction reaches a finite limit; $\tilde{\tau}_2^{(0)}$ becomes relatively uniform with $\tilde{Z}$. The total stress is now dominated by $\tilde{\tau}_2^{(0)}(\bar{\Gamma}_2)$ which is proportional to the water layer thickness in the top aquifer, i.e.

$$\tilde{\tau}_2^{(0)}(\bar{\Gamma}_2) = \tilde{\sigma}_2^{(0)}(\bar{\Gamma}_2) - \tilde{p}'(\bar{\Gamma}_2) = \tilde{\sigma}_2^{(0)}(\bar{\Gamma}_2) - (\tilde{h}^{(0)} - \tilde{b}_2') = -\bar{n}_3(\tilde{h}^{(0)} - \tilde{b}_2'). \tag{12.1}$$

(*c*) *Transient pumping*

Four different patterns of pumping, shown in figure 10*a–d*, are considered with a view to examining their possible hysteretic effect on subsidence. In the aquitard we have chosen $C_c = 6.0$ for virgin compression and $C_c' = 0.2C_c = 1.2$ for swelling and recompression. All time histories are shown for $\tilde{R} = 0.2$ which is representative of the neighbourhood of the well.

(i) *Steady against intermittent pumping*

We compare here two cases sharing the same average pumping rate as shown in figure 10*a*. In the first case $\tilde{Q}(\tilde{T})$ is cyclic, being a constant $\tilde{Q}(\tilde{T}) = 1.0$ for the first half of a cycle $0 < \tilde{T} < 0.5$ and zero for the second half $0.5 < \tilde{T} < 1$, etc. The curve of

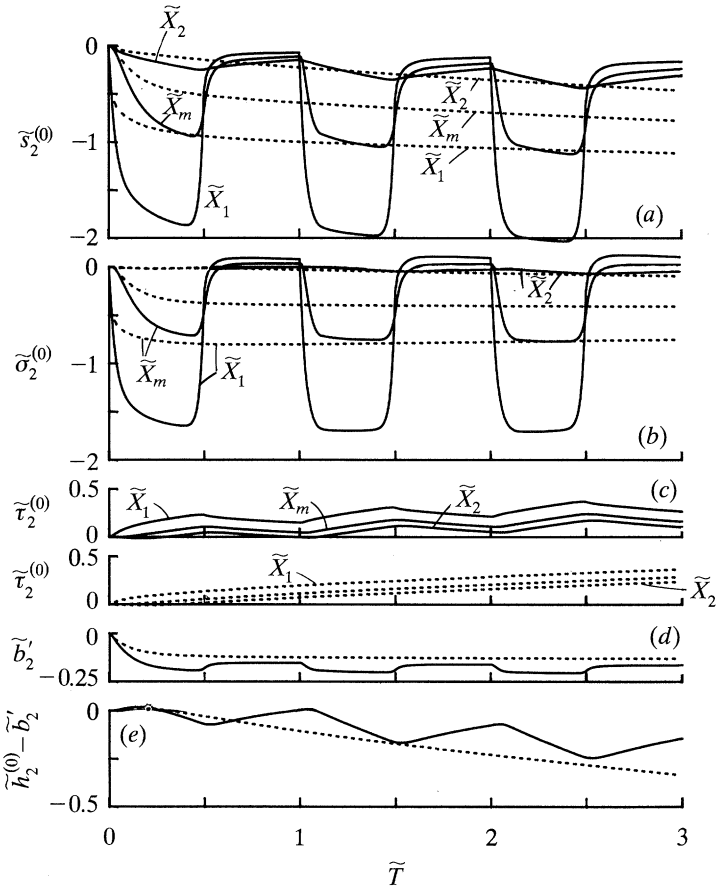

Figure 11. Time variations of (*a*) $\tilde{s}_2^{(0)}$, (*b*) $\tilde{\sigma}_2^{(0)}$, (*c*) $\tilde{\tau}_2^{(0)}$, and (*d*) $\tilde{b}_2'$, (*e*) $\tilde{h}^{(0)}-\tilde{b}_2'$ for $\tilde{R}=0.2$. Steady (solid) and intermittent (dashed), by pumping depicted in figure 10*a*.

stress against void ratio necessarily branches off from virgin compression to swelling and recompression, etc. In the second case water is drawn steadily at the average rate of $\tilde{Q}(\tilde{T})=0.5$. The soil undergoes virgin compression monotonically. Time variations of $\tilde{s}_2^{(0)}(\bar{\Gamma}_2)$, $\tilde{\sigma}_2^{(0)}$ and $\tilde{\tau}_2^{(0)}$ at $\tilde{R}=0.2$ and three depths $\tilde{X}=\tilde{X}_1$, $\tilde{X}=\tilde{X}_m=\frac{1}{2}(\tilde{X}_1+\tilde{X}_2)$ and $\tilde{X}_2$ are shown in figure 11*a* and *b*. The level $\tilde{X}_m$ is slightly below the initial mid-level of the aquitard because the initial void ratio distribution is not uniform (see (5.11) and figure 2*a*), but is representative of the centre portion of the aquitard. Note that the changes in both the drawdown and the effective stress recover from large negative values to nearly zero as soon as pumping stops. The reason that $\tilde{\sigma}^{(0)}$ is slightly positive (tension) is associated with the small swelling index C_c'. As a consequence the second integral in (9.7), which is positive becomes more dominant than $\tilde{s}_2^{(0)}(\bar{\Gamma}_2)$. Except for the change in total stress all quantities behave drastically differently in the two cases. In particular, the ground subsidence by cyclic pumping is considerably greater than that by uniform pumping at all $\tilde{T}$ as shown in figure 11*d*. To lessen subsidence, it is therefore better to pump steadily rather than intermittently over a long time.

The history of the water table level outside the well region at $\tilde{R}=0.2$ is shown in figure 11*e*. Notice again the initial rise in both cases (Mandel–Cryer effect). For large

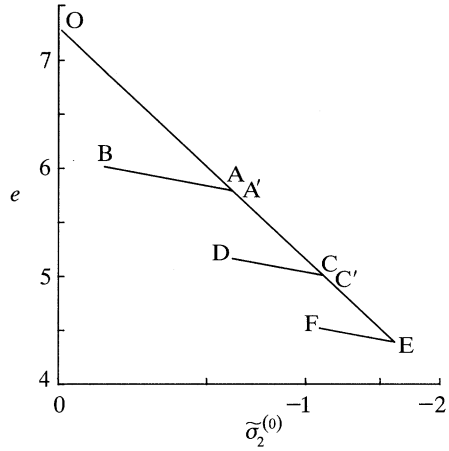

Figure 12. The void ratio against effective stress diagram $C_c = 6.0$ at $\tilde{R} = 0.2$ on $\bar{\Gamma}_1$.

$\tilde{T}$, the water table drops more rapidly and steadily when pumping is steady. Therefore for maintaining the water table close to the ground surface, intermittent pumping appears more preferable.

(ii) *Cyclically modulated pumping*

The pumping rate varies sinusoidally in time according to $\tilde{Q}(\tilde{T}) = \tilde{T} + \sin \tilde{T}$. This case partly resembles the one-dimensional model for Pixley, California, by Helm (1975, 1976) and by Narasimhan & Witherspoon (1978), who assumed a surface load varying similarly in time. Figure 12 shows the computed e_2 against $\log_{10}(-\tilde{\sigma}_2^{(0)})$ curve at a point $\tilde{R} = 0.2$ on $\bar{\Gamma}_1$. The letter symbols correspond to peaks and troughs of $\tilde{Q}(\tilde{T})$ marked in figure 10*b*. At the start of pumping $\tilde{\sigma}_2^{(0)}$ decreases (i.e. compression increases) and the variation of e_2 against $\log_{10}(-\tilde{\sigma}_2^{(0)})$ follows the virgin compression line O–A in figure 12. When $\tilde{Q}(\tilde{T})$ decreases, $\tilde{\sigma}_2^{(0)}$ increases (swelling) and the curve is shown by line A–B in figure 12. As $\tilde{Q}(\tilde{T})$ increases from B to A′ in figure 10*b*, the corresponding curve in figure 12 follows the recompression line BA′. Upon passing beyond the point A′, $\tilde{\sigma}_2^{(0)}$ becomes smaller than that at A′ which is the maximum compression so far experienced by the soil. Therefore the stress state returns to virgin compression and onto the path A′C which is the extension of OA. For the rest of $\tilde{Q}(\tilde{T})$ in figure 10*b*, the stress state follows CD, DC′, C′E, and EF, etc. The time histories of drawdown, the pumping induced changes in the effective stress and in the total stress, as well as the ground subsidence are similar to the history of pumping, as shown in figure 13*a–d*. Despite the substantial changes of $\tilde{\sigma}_2^{(0)}$ over AB, CD, EF in figure 12, the ground surface rebounds only slightly after each cycle due to the relatively small change of e_2 in the swelling–recompression process (see figure 13*d*).

The water table level at $\tilde{R} = 0.2$ is presented in figure 13*e*, showing an expected initial rise and eventual fall, with undulations. Except for this Mandel–Cryer effect which is a three-dimensional phenomenon, these results are qualitatively consistent with the one-dimensional models of Helm (1976) and of Narasimhan & Witherspoon (1978).

(iii) *Pumping and recharging*

Let all the water pumped out during the first phase be reinjected slowly into the artesian aquifer, as shown in figure 10*c*. At the end of $\tilde{T} = 3$ the net water removal

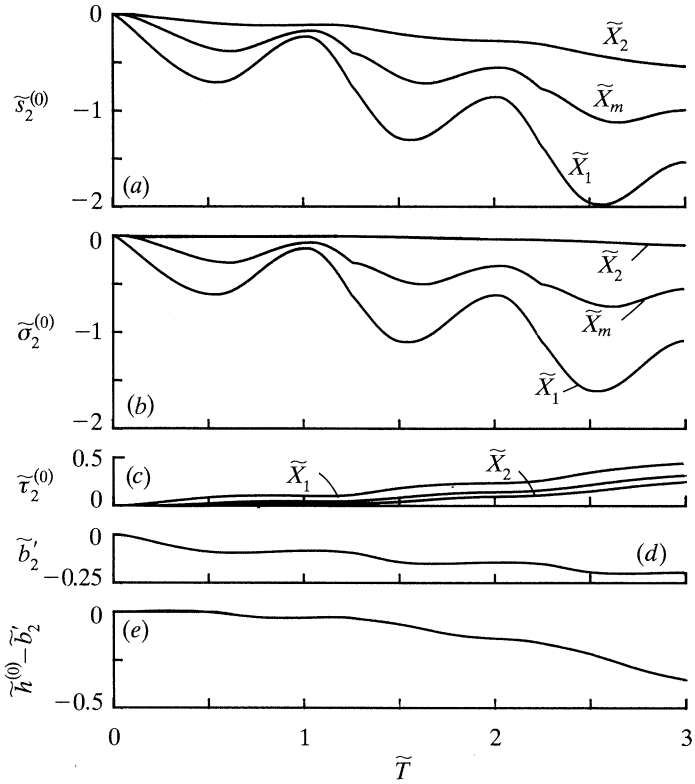

Figure 13. Time variations of (*a*) $\tilde{s}_2^{(0)}$, (*b*) $\tilde{\sigma}_2^{(0)}$, (*c*) $\tilde{\tau}_2^{(0)}$, (*d*) $\tilde{b}_2'$, (*e*) $\tilde{h}^{(0)}-\tilde{b}_2'$ for $R = 0.2$ by cyclically modulated pumping depicted in figure 10*b*.

is zero. As in previous cases, sample time histories of $\tilde{s}_2^{(0)}, \tilde{\sigma}_2^{(0)}, \tilde{\tau}_2^{(0)}$ at three depths and $\tilde{R} = 0.2$ are shown in figure 14. Their pattern is similar to that of $\tilde{Q}(\tilde{T})$. Note, in particular, that $\tilde{s}_2^{(0)}(\bar{\Gamma}_2)$ rises rapidly to a positive value as soon as reinjection starts. $\tilde{\sigma}_2^{(0)}(\bar{\Gamma}_2)$ becomes positive (tension) after $\tilde{T} = 1.5$ because of prolonged injection, while the sum $\sigma_2^{(0)} = \bar{\sigma}_2^{(0)} + \tilde{\sigma}_2^{(0)}$ is still compressive, though reduced in magnitude. Using the same reasoning given for Case (i), it follows from (9.1) that $\tilde{H}_0 - \tilde{H}$ becomes positive. Therefore the water table rises above the initial level at $\tilde{Z} = \tilde{H}$ and the thickness of the dry zone in the phreatic aquifer becomes less than $\frac{1}{2}$. The total stress change $\tilde{\tau}_2^{(0)}(\bar{\Gamma}_2)$ shown in figure 14*c* becomes negative after $\tilde{T} = 0.8$. This negativeness (increased compression) results from the increased buoyancy induced by the rise of the water table above its initial level $\tilde{H}$. Thus the combined weight of both the solid and the fluid above the upper interface is increased from the initial state. As is obvious in figure 14*d*, at the end $\tilde{T} = 3$ when all the pumped water is reinjected, the ground level does not return to the initial position. Combined with the significant increase of $\tilde{s}_2^{(0)}(\bar{\Gamma}_2)$, this explains why the water table also rises by a large amount for large time.

(iv) *Cyclic pumping and recharging*

Water is pumped at the rate $\tilde{Q} = 1$ during the first half of each cycle and recharged at the rate $\tilde{Q} = -0.2$ during the second half. The low rate of recharge is chosen so as to avoid liquefaction anywhere in the soil in the entire computation, i.e. to keep the

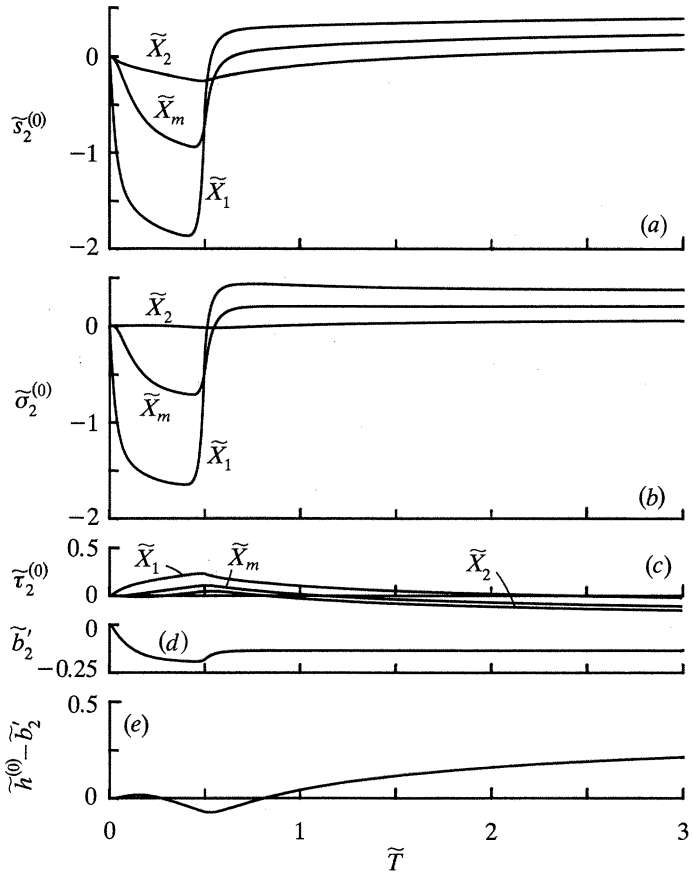

Figure 14. Time variations of (*a*) $\tilde{s}_2^{(0)}$, (*b*) $\tilde{\sigma}_2^{(0)}$, (*c*) $\tilde{\tau}_2^{(0)}$ and (*d*) $\tilde{b}_2'$, (*e*) $\tilde{h}^{(0)}-\tilde{b}_2'$ at $\tilde{R}=0.2$ by pumping and recharging depicted in figure 10*c*.

sign of $\tilde{\sigma}=\tilde{\bar{\sigma}}+\tilde{\sigma}'$ negative (compression) throughout the computation so that (2.17) remains valid.

The aquitard drawdowns at three levels $\tilde{X}_1, \tilde{X}_m=(\tilde{X}_1+\tilde{X}_2)$ and $\tilde{X}_2$ for $\tilde{R}=0.2$ are shown in figure 15*a*. During the recharging phase of the first cycle, the vertical distribution of $\tilde{s}_2^{(0)}$ is reversed and the flow direction in the aquitard becomes upward, as in Cases (i) and (iii). In the second ($1.0<\tilde{T}<2.0$) and third ($2.0<\tilde{T}<3.0$) cycles the same kind of variation of $\tilde{s}_2^{(0)}$ is repeated. The amplitude of $\tilde{s}_2^{(0)}$ is quite large. In figure 15*b*, the effective stress variation is shown for the same settings. During injections, most part of the vertical cross section is in tension as compared to the initial state, since $\tilde{\sigma}_2^{(0)}>0$. The vertical settlement is shown in figure 15*d*. Hysteresis is obvious after the first pumping period. While $\tilde{\sigma}_2^{(0)}$ fluctuates greatly, the ground level recovers only slightly. The water table recovers significantly after each cycle, as shown in figure 15*e*.

13. Concluding remarks

When water is pumped into an isolated well in a soil stratum consisting of alternating sand and clay layers, the pore fluid seeks the path of least resistance by flowing transversely in the clay layers and longitudinally in the sand layers. On the other hand soil deformation is primarily one dimensional in the transverse direction

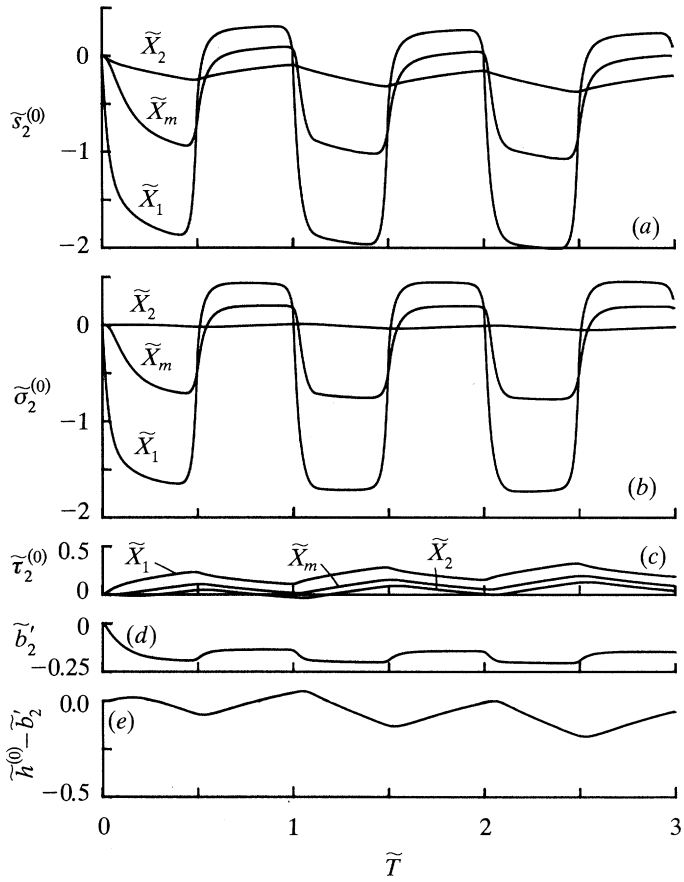

Figure 15. Time variations of (*a*) $\tilde{s}_2^{(0)}$, (*b*) $\tilde{\sigma}_2^{(0)}$, (*c*) $\tilde{\tau}_2^{(0)}$ and (*d*) $\tilde{b}_2'$, (*e*) $\tilde{h}^{(0)}-\tilde{b}_2'$ at $\tilde{R}=0.2$ by cyclic pumping and recharging depicted in figure 10*d*.

only. These physical features have been recognized before and utilized in existing papers by well hydrologists and geotechnical engineers. However, combination of the two have been made in existing work only in an *ad hoc* manner. In this paper we have shown by a systematic perturbation analysis that such a combination is indeed correct with an error of $O(\delta^{\frac{1}{2}})$ is subsidence and $O(\delta)$ in drawdown, where δ is the small ratio of permeabilities, under the stated assumptions. In addition, fluid drawdown and effective soil stress are in general coupled nonlinearly, and the total stress is no longer constant in depth. With a constitutive model representing the well-known nonlinear and hysteretic behaviour of soft soils we have examined the effect of pumping from an isolated well on the finite displacement of the ground surface and the water table, as well as the transient evolution of the drawdown in various parts of the soil. Our results for steady pumping displays Mandel–Cryer effect which has so far been predicted only for infinitesimal soil strain in well hydraulics and for finite strain in a simple sphere. Examples for transient pumpings (intermittent or cyclic pumping and recharging) show that the ground surface and the water table can respond in interesting manners which are relevant to the planning or operation of wells. In all examples the common approximation of constant total stress is found to be not quite accurate.

Extension of the present theory to allow finite compressibilities in all layers is straightforward and worthwhile. Since for a single well the physics is already highly nonlinear, the interaction between two or more adjacent wells or concentrated zones of pumping, separated by distances comparable to the typical radius of influence, cannot be treated by superposition, neither is the combined effect of pumping and surface loading. While the present theory allows large displacement of the water table within the original phreatic aquifer, modifications are needed to deal with the more dramatic case where the water table can move across several soil layers. For these complex problems, further research is worthwhile.

We thank the Solid and Geomechanics Program, U.S. National Science Foundation, for supporting this research through Grant MSM 8616693.

Appendix A. Linearized Biot's equations of poroelasticity

The linearized equation of mass conservation for the solid is

$$-\partial n'/\partial t+\nabla\cdot((1-\bar{n})\,\boldsymbol{v}_{\mathrm{s}}')=0, \tag{A 1}$$

while the equilibrium equation is

$$\nabla\cdot\sigma'=\nabla p'+(\rho_{\mathrm{s}}-\rho_{\mathrm{w}})\,\boldsymbol{g}n'. \tag{A 2}$$

For infinitesimal stress and strain Hooke's law applies

$$\partial\sigma'(\boldsymbol{x},t)/\partial t=\bar{G}(\nabla\boldsymbol{v}_{\mathrm{s}}'+\nabla\boldsymbol{v}_{\mathrm{s}}'^{\mathrm{T}})+(\bar{D}-2\bar{G})\,\nabla\cdot\boldsymbol{v}_{\mathrm{s}}'\boldsymbol{I}, \tag{A 3}$$

where $\nabla\boldsymbol{v}_{\mathrm{s}}'^{\mathrm{T}}$ denotes the transpose of $\nabla\boldsymbol{v}_{\mathrm{s}}'$, and $\bar{G}$ and $\bar{D}$ are the shear modulus and constrained modulus respectively. The time derivative of (A 2) then reads

$$\nabla\cdot\partial\sigma'/\partial t=\nabla\,\partial p'/\partial t+(\rho_{\mathrm{s}}-\rho_{\mathrm{w}})\,\boldsymbol{g}\,\partial n'/\partial t, \tag{A 4}$$

or, by combining with (A 3)

$$\nabla\cdot[\bar{G}(\nabla\boldsymbol{v}_{\mathrm{s}}'+(\nabla\boldsymbol{v}_{\mathrm{s}}')^{\mathrm{T}})+(\bar{D}-2\bar{G})\,\nabla\cdot\boldsymbol{v}_{\mathrm{s}}'\boldsymbol{I}]=\rho_{\mathrm{w}}g\,\nabla\,\partial s'/\partial t+(\rho_{\mathrm{s}}-\rho_{\mathrm{w}})\,\boldsymbol{g}\nabla\cdot[(1-\bar{n})\,\boldsymbol{v}_{\mathrm{s}}']. \tag{A 5}$$

For an axisymmetric problem let u and w be the radial and vertical velocity components of the solid phase in the r and z directions. Equation (A 5) may be written for each layer, as follows,

$$\frac{\partial}{\partial r}\left[\bar{D}\frac{1}{r}\frac{\partial ru'}{\partial r}+(\bar{D}-2\bar{G})\frac{\partial w'}{\partial z}\right]+\frac{\partial}{\partial z}\left(\bar{G}\frac{\partial u'}{\partial z}+\bar{G}\frac{\partial w'}{\partial r}\right)=\rho_{\mathrm{w}}g\frac{\partial^2 s'}{\partial r\,\partial t}, \tag{A 6}$$

$$\frac{1}{r}\frac{\partial}{\partial r}r\left[\bar{G}\frac{\partial u'}{\partial z}+\bar{G}\frac{\partial w'}{\partial r}\right]+\frac{\partial}{\partial z}\left[(\bar{D}-2\bar{G})\frac{1}{r}\frac{\partial ru'}{\partial r}+\bar{D}\frac{\partial w'}{\partial z}\right]=\rho_{\mathrm{w}}g\frac{\partial^2 s'}{\partial z\,\partial t}$$

$$+\frac{1}{r}\frac{\partial}{\partial r}r[-g(\rho_{\mathrm{s}}-\rho_{\mathrm{w}})(1-\bar{n})\,u']+\frac{\partial}{\partial z}[-g(\rho_{\mathrm{s}}-\rho_{\mathrm{w}})(1-\bar{n})\,w']. \tag{A 7}$$

Appendix B. Derivation of (7.21)

The lagrangian equilibrium equations in the phreatic aquifer are

$$\frac{\partial}{\partial Z'}(\tilde{\bar{\sigma}}+\tilde{\sigma}_3')=(1-\bar{n}_3)\frac{\rho_{\mathrm{s}}}{\rho_{\mathrm{w}}}+O(\delta) \tag{B 1}$$

in the dry zone, and

$$\frac{\partial}{\partial Z'}(\tilde{\bar{\sigma}}+\tilde{\sigma}'_3)=(1-\bar{n}_3)\left(\frac{\rho_s}{\rho_w}-1\right)+O(\delta) \tag{B 2}$$

in the wet zone. We next integrate (B 1) from the instantaneous water table to the ground surface

$$-[\tilde{\bar{\sigma}}_3+\tilde{\sigma}'_3]_{\bar{\Gamma}_H}=(1-\bar{n}_3)(\rho_s/\rho_w)(\tilde{B}_1+\tilde{B}_2+\tilde{B}_3-\tilde{H}_o) \tag{B 3}$$

and integrate (B 2) from $\bar{\Gamma}_2$ to the water table:

$$[\tilde{\bar{\sigma}}_3+\tilde{\sigma}'_3]_{\bar{\Gamma}_H}-[\tilde{\bar{\sigma}}_3+\tilde{\sigma}'_3]_{\bar{\Gamma}_2}=(1-\bar{n}_3)(\rho_s/\rho_w-1)(\tilde{H}_o-\tilde{B}_1-\tilde{B}_2). \tag{B 4}$$

Adding the preceeding two equations we obtain

$$-[\tilde{\bar{\sigma}}_3+\tilde{\sigma}'_3]_{\bar{\Gamma}_2}=(1-\bar{n}_3)(\rho_s/\rho_w)\tilde{B}_3-(1-\bar{n}_3)(\tilde{H}_o-\tilde{B}_1-\tilde{B}_2). \tag{B 5}$$

Since at $\tilde{T}=0$, $\tilde{\sigma}'_3=0$ and $\tilde{H}=\tilde{H}_o$, it follows that

$$-\tilde{\bar{\sigma}}_3(\bar{\Gamma}_2)=(1-\bar{n}_3)(\rho_s/\rho_w)\tilde{B}_3-(1-\bar{n}_3)(\tilde{H}-\tilde{B}_1-\tilde{B}_2). \tag{B 6}$$

Subtracting (B 6) from (B 5) we get

$$-\tilde{\sigma}'_3(\bar{\Gamma}_2)=(1-\bar{n}_3)(\tilde{H}-\tilde{H}_o), \tag{B 7}$$

which is (7.21), by virtue of stress continuity.

Appendix C. List of symbols

In all subscripted variables the range of i is always $i=1,2,3$.

a	well radius
a_v	coefficient of soil compressibility
B_i	initial depth of ith soil layer
b_i	instantaneous depth of ith soil layer
C_c	compression index of clay aquitard
C'_c	swelling and recompression index of aquitard
D_i	constrained modulus of soil
e_i	void ratio
$\boldsymbol{e}_r, \boldsymbol{e}_z$	unit vectors along the radial and vertical directions
G	shear modules of soil
g	gravity
H	initial height of the water table
h	instantaneous height of the water table
J	jacobian determinant
k_i	hydraulic conductivity of ith soil layer
M	number of grid points along X-axis
N	number of grid points along η-axis
n_i	porosity of ith soil layer
p	pore pressure
$Q(t)$	pumping rate
R, r	lagrangian and eulerian radial coordinate
T, t	lagrangian and eulerian time
u_i	radial component of solid velocity of ith soil layer
$\boldsymbol{v}_s, \boldsymbol{v}_w$	velocity vectors for solid and fluid
w_i	vertical component of solid velocity of ith soil layer
X	reduced vertical coordinate (cf. (5.11))
x, y, z	eulerian cartesian coordinates
β	bulk modulus of soil
Γ_H	water table
Γ_i	top surface of ith layer
δ	small parameter (cf. (3.5b))
η	logarithmic coordinate along r-axis ($=\ln R/a$)
κ	ratio of depth-averaged hydraulic conductivities of aquifers ($=\hat{k}_1/\hat{k}_3$)
λ	Lamé constant
ν	measure of drawdown to layer thickness ($=\hat{s}/\hat{b}$)
ρ	density
σ_{ij}	effective stress tensor
τ_{ij}	total stress tensor
$\bar{(\ )}$	initial state
$(\ )'$	perturbation from initial state
$\hat{(\ )}$	scale of physical variable

s_i	drawdown	$(\tilde{\ })$	dimensionless variable
$\mathscr{S}_T$	storage coefficient of aquitard ($= \rho_w g \hat{b}/\hat{D}_2$)	$(\ )^n$	nth order term in perturbation solution ($n = 0, 1, 2 \ldots$).

References

Bear, J. 1972 *Dynamics of fluids in porous media*. New York: Elsevier.

Bear, J. 1979 *Hydraulics of groundwater*. New York: McGraw-Hill.

Bear, J. & Corapcioglu, M. Y. 1981*a* Mathematical model for regional land subsidence due to pumping. I: Integrated aquifer subsidence equations based on vertical displacement only. *Wat. Resour. Res.* **17**, 937–946.

Bear, J. & Corapcioglu, M. Y. 1981*b* Mathematical model for regional land subsidence due to pumping. II: Integrated aquifer subsidence equations for vertical and horizontal displacements. *Wat. Resour. Res.* **17**, 947–958.

Bolt, B. A., Horn, W. L., Macdonald, G. A. & Scott, R. F. 1977 *Geological hazards*. Springer-Verlag.

Bredehoeft, J. D. & Pinder, G. F. 1970 Digital analysis of areal flow in multiaquifer groundwater systems: a quasi three-dimensional model. *Wat. Resour. Res.* **6**, 883–888.

Cooper, H. H. 1966 The equation of groundwater flow in fixed and deforming coordinates. *J. geophys. Res.* **71**, 4785–4790.

Corapcioglu, M. Y. & Bear, J. 1983 A mathematical model for regional land subsidence due to pumping. III. Integrated equations for a phreatic aquifer. *Wat. Resour. Res.* **19**, 895–908.

Corapcioglu, M. Y. & Brutsaert, W. 1977 Viscoelastic aquifer model applied to subsidence due to pumping. *Wat. Resour. Res.* **13**, 597–604.

Cryer, C. W. 1963 A comparison of the three-dimensional consolidation theories of Biot and Terzaghi. *Q. Jl Mech. appl. Math.* **16**, 401–412.

De Josselin de Jong, G. 1963 Considatie in drie dimensies, LGM. *Mededelingen* **7**, 57–73.

Fallou, S. N., Mei, C. C. & Lee, C. K. 1991 Subsidence due to pumping from a layered soil – a perturbation theory. *Int. J. numer. Analysis Meth. Geomech.* (In the press.)

Gambolati, G. A. 1973*a* Equation for one-dimensional vertical flow of groundwater. 1. The rigorous theory. *Wat. Resour. Res.* **9**, 1022–1028.

Gambolati, G. A. 1973*b* Equation for one-dimensional vertical flow of groundwater. 2. Validity range of the diffusion equation. *Wat. Resour. Res.* **9**, 1385–1395.

Gambolati, G. A. & Freeze, R. A. 1973 Mathematical simulation of the subsidence of Venice. I. Theory. *Wat. Resour. Res.* **9**, 721–733.

Gambolati, G. A., Gatto, P. & Freeze, R. A. 1974 Mathematical simulation of the subsidence of Venice. 2. Results. *Wat. Resour. Res.* **10**, 563–577.

Gambolati, G. A., Sartoretto, F. & Uliana, F. 1986 A conjugate gradient finite element model of flow for large multiaquifer systems. *Wat. Resour. Res.* **22**, 1003–1015.

Gibson, R. E., England, G. L. & Hussey, M. J. L. 1967 The theory of one-dimensional consolidation of saturated clays. I. Finite nonlinear consolidation of thin homogeneous layers. *Geotechnique* **17**, 261–273.

Gibson, R. E., Gobert, A. & Schiffman, R. L. 1989 On Cryer's problem with large displacements. *Int. J. numer. Analysis Meth. Geomech.* **13**, 251–262.

Gibson, R. E., Schiffman, R. L. & Cargill, K. W. 1981 The theory of one-dimensional consolidation of saturated clays. II. Finite nonlinear consolidation of thick homogeneous layers. *Can. geotech. J.* **18**, 280–293.

Hantush, M. S. 1960 Modification of the theory of leaky aquifers. *J. geophys. Res.* **65**, 3713–3725.

Hantush, M. S. & Jacob, C. E. 1954 Plane potential flow of ground water with linear leakage. *Trans. Am. Geophys. Union* **35**, 917–936.

Hantush, M. S. & Jacob, C. E. 1955*a* Nonsteady radial flow in an infinite leaky aquifer. *Trans. Am. Geophys. Union* **36**, 95–100.

Hantush, M. S. & Jacob, C. E. 1955*b* Steady three dimensional flow to a well in a two-layered aquifer. *Trans. Am. Geophys. Union* **36**, 286–292.

PHILOSOPHICAL TRANSACTIONS OF THE ROYAL SOCIETY A MATHEMATICAL, PHYSICAL & ENGINEERING SCIENCES

Helm, D. C. 1975 One-dimensional simulation of aquifer system compaction near Pixley, California. 1. Constant parameters. *Wat. Resour. Res.* **11**, 465–478.

Helm, D. C. 1976 One-dimensional simulation of aquifer system compaction near Pixley, California. 2. Stress dependent parameters. *Wat. Resour. Res.* **12**, 375–391.

Herrera, I. & Figueroa, G. E. 1969 A correspondence principle for the theory of leaky aquifers. *Wat. Resour. Res.* **5**, 900–904.

Holtz, R. D. & Kovacs, W. D. 1981 *An introduction to geotechnical engineering*, p. 342. New Jersey: Prentice Hall.

Javandel, I. J. & Witherspoon, P. A. 1969 A method of analyzing transient fluid flow in multilayered aquifers. *Wat. Resour. Res.* **5**, 856–869.

Lambe, T. W. 1951 *Soil testing for engineers*, p. 84. New York: Wiley.

Lambe, T. W. & Whitman, R. V. 1969 *Soil mechanics*. New York: Wiley.

Mandel, J. 1953 Consolidation des sols (étude mathematique). *Geotechnique* **3**, 287–299.

Marsal, R. J. 1957 Unconfined compression and vane shear tests in volcanic Incastrine clays. *ASTM Spec. Tech. Publ.* **232**, 229–241.

Narasimhan, T. N. & Witherspoon, P. A. 1977 Numerical model for saturated unsaturated flow in deformable porous media. 1. Theory. *Wat. Resour. Res.* **13**, 657–664.

Narasimhan, T. N. & Witherspoon, P. A. 1978 Numerical model for saturated unsaturated flow in deformable porous media. 3. Application. *Wat. Resour. Res.* **14**, 1017–1034.

Neuman, S. P. & Witherspoon, T. N. 1969*a* Theory of flow in a confined two-aquifer system. *Wat. Resour. Res.* **5**, 803–816.

Neuman, S. P. & Witherspoon, P. A. 1969*b* Applicability of current theories of flow in leaky aquifers. *Wat. Resour. Res.* **5**, 817–829.

Poland, J. F. & Davis, G. H. 1969 Land subsidence due to withdrawal of fluids. *Rev. Engng Geology* **2**, 187–269.

Rudoph, D. L. & Frind, E. O. 1991 Hydraulic response of highly compressible aquitards during consolidation. *Wat. Resour. Res.* **27**, 17–30.

Smiles, D. E. & Rosenthal, M. J. 1968 The movement of water in swelling materials. *Austr. J. Soil Res.* **6**, 237–248.

Verruijt, A. 1969 Elastic storage of aquifers. In *Flow through porous media* (ed. R. M. deWiest). Academic Press.

Zeevaert, L. 1983 *Foundation engineering for difficult subsoil conditions*, 2nd edn (676 pages). Van Nostrand Reinhold.

Received 25 March 1991; revised 10 September 1991; accepted 14 October 1991

PHILOSOPHICAL TRANSACTIONS OF THE ROYAL SOCIETY A MATHEMATICAL, PHYSICAL & ENGINEERING SCIENCES